
**Politecnico di Torino**

**Corso di Laurea Magistrale in Ingegneria Biomedica**

# Comparison of the primary stability of different acetabular cups considering various acetabular bone defect sizes using a cup-block model

Author:
Vittoria Civilini

Supervisors:
Prof. Cristina Bignardi
Dr. Mara Terzini
Prof. Rainer Bader
M. Sc. Christian Schulze

07/07/2020

# Index

# Abbreviation list

| | |
|---|---|
| THA | Total Hip Arthroplasty |
| OA | Osteoarthritis |
| ASA | American Society of Anesthesiologists |
| AAOS | American Academy of Orthopedic Surgeons |
| CT | Computed Tomography |
| TM | Trabecular Metal™ |
| PMI | Polyimide |
| PVC | Polyvinylchloride |
| PU | Polyurethane |
| FE | Finite Elements |
| CNC | Computer numerical control |
| RP | Reference point |

# Abstract

Total hip arthroplasty (THA) is currently one of the most widely performed surgical interventions due to its high rate of success. However, surgical failures still occur and can lead to severe consequences. The main cause of implant failure is aseptic loosening, often related to a deficient osseointegration of the implant and osteolysis. Therefore, a good primary stability is mandatory in order to achieve bone ingrowth and long-term implant stability. Initial stability may be influenced by the type of implant fixation (e.g. press-fit or adjunctive screw fixation), the surgical approach, the presence of bone defects, and bone quality. In press-fit acetabular cups, the primary stability is achieved through frictional forces by inserting the cup in an under-reamed cavity. As a consequence, the bone-implant contact area highly affects primary stability. In the presence of acetabular defects, the effective contact area can be extremely reduced and the choice of the most suitable implant (e.g. primary cup, revision cup, reinforcement cage) can drastically affect the cup stability. Hence, the aim of this Thesis is to study and compare the initial stability of a primary acetabular cup and a revision cup in three types of bone substitute blocks (Sawbones® Pacific Research Laboratories, Inc., Vashon, USA) characterized by different defect sizes, milled in the blocks using a CNC-machine. The influence of the defect size on primary stability was investigated both experimentally and numerically using a finite elements (FE) model. The latter was used as well to characterize the influence of blocks' density.

A lever-out test was carried out and five replicas were performed for each combination of the acetabular cup and block type. Preliminary insertion tests were performed to determine the seating position of the cup by means of a static universal testing machine (Zwick/Roell Z050, Zwick GmbH & Co. KG, Ulm, Germany) under load-controlled conditions. Push-in and lever-out tests were performed out under displacement-controlled conditions at a crosshead velocity of 20 mm/min with the same static testing machine. The data obtained in all the tests were computed using MATLAB 2017b (MathWorks Inc., Natick, MA, USA). Push-in force, lever-out moment, lever-out work, and interface stiffness determined for each trial were compared to delineate the cups' behavior in the different blocks. We found a decrease in all the parameters as the extension of the defect increased, and generally better results were achieved by the TM™ cup. A statistical analysis was performed to investigate whether the different types of implant (primary or revision cup) and the presence and the size of the defects, determine significant differences in the aforementioned parameters used to assess primary stability. A Welch-ANOVA test, followed by a Games-Howell post hoc test, was

conducted on the push-in forces, the lever-out moments, and the interface stiffnesses. A One-Way ANOVA, followed by a Bonferroni post hoc test, was operated on the lever-out work. Statistical significance was established between the two cups for all the larger defect parameters except the interface stiffness. Furthermore, the influence of the defect size on the primary stability of the cups was confirmed.

The FE cup-block model for the intact cavity was validated using the experimental test results from a previous work, performed with the SeleXys PC® acetabular cup. We found a maximum difference of 33% in the push-in forces between the previously obtained experimental data and the FE model. The push-in force, the lever-out moment, and the interface stiffness of the cup-block FE models with the two different defects sizes were compared to the ones of the intact model in order to establish the influence of defects in the primary stability. All the extracted parameters show a strong dependence on both the defect size and the blocks' material density. Moreover, the initial cup stability decreases with an increase of the defect size and with a decrease in the density. The analysis of the contact area demonstrated that the contact between the cup and its substrate is localized on a narrow surface near the equator of the cavity. The influence of the contact area between the cup and the bone on the primary stability was also investigated. A direct correlation between the contact area and all the all parameters (i.e. push-in force, lever-out moment, and interface stiffness) was determined.

The results of this Thesis can be used in future works for the development of a FE model for the revision acetabular cup, in order to further investigate the influence of the type of implant on the primary stability in the presence of acetabular defects.

# 1. Introduction

## 1.1 Hip joint

### 1.1.1 Anatomy and diseases

The hip joint is a ball on socket joint, formed by an articulation between the head of the femur and the pelvic acetabulum. The acetabulum is a cup-shaped structure and is formed by the three bones of the pelvis: ilium, ischium, and pubis. The femur head is two-third of a sphere that fits into the acetabular concavity.[1] Both, the acetabulum and the head of the femur, are covered by articular cartilage, which acts with the synovial fluid as a cushion to help to reduce friction. The depth of acetabulum is further increased by a fibrocartilaginous collar - the acetabular labrum that adds stability to the hip joint. The stability is also achieved through the bony structure, the capsule, the ligaments (intracapsular and extracapsular) and the surrounding muscles and is also an essential characteristic for weight-bearing function.[2] Figure 1.1 represents a scheme of hip joint anatomy.

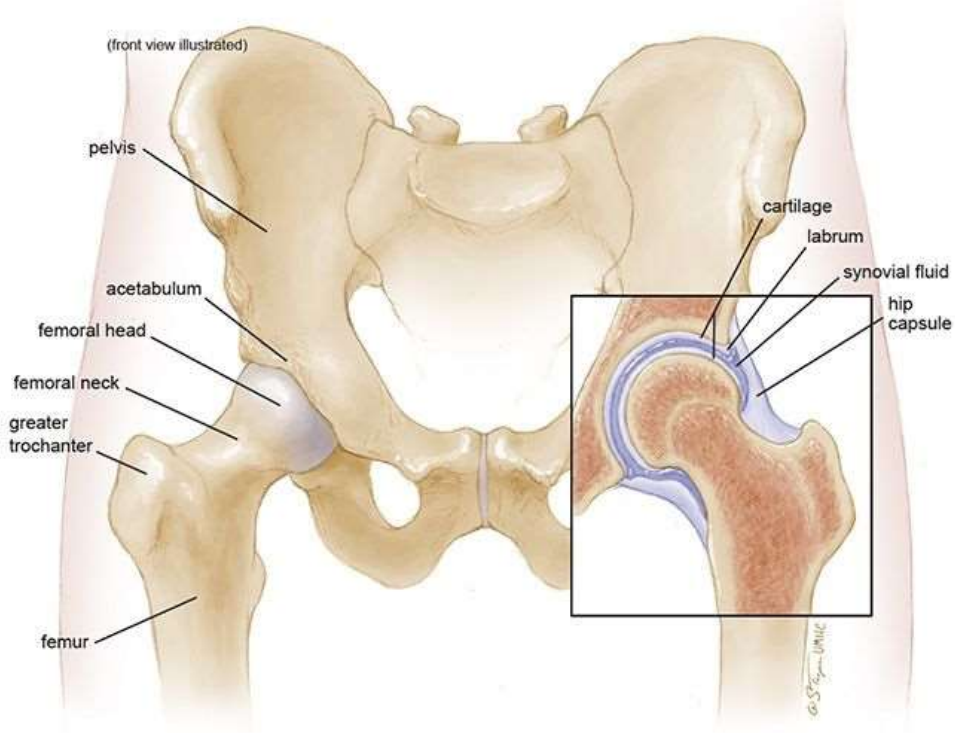


*Figure 1.1 – Right: overview of the hip joint and the surrounding bony structure. Left: depiction of the articulating parts of the acetabular joint.*[3]

The hip is prone to several types of pathologies that can be divided into different categories: soft tissue disorders, joint disorders, osseous disorders, fractures, dislocations, and pediatric disorders. Some of them can be treated with pharmacological and conservative treatments. Nonpharmacological methods include patient education and rehabilitation.[4] If medications and other treatments prove to be insufficient, a surgical approach should be used as the last

instance. The most common hip surgery is total hip arthroplasty (THA), a procedure in which a worn out or damaged hip joint is replaced with an endoprosthesis.

The most frequent reason for hip replacement is osteoarthritis (OA) which is a degenerative type of arthritis characterized by a gradual deterioration of articular cartilage. The degenerative process occurs with a reparative process with reactive bone formation, generation of osteophytes, and bone remodeling. Figure 1.2 shows a schematic view of OA damages.

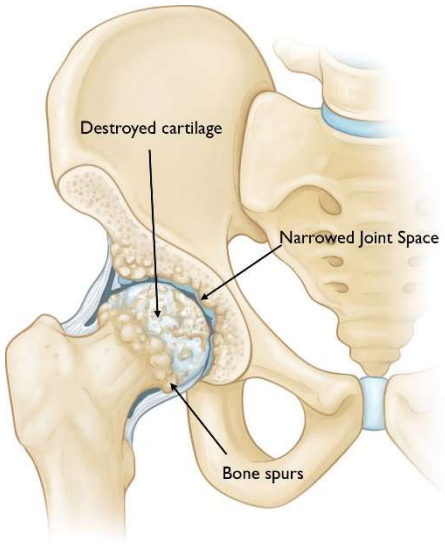


*Figure 1.2 – Hip OA damages: degenerated cartilage, narrowed joint space, and bone spurs.* [5]

OA can be divided into primary and secondary types. Primary OA is of idiopathic origin and usually affects multiple joints whereas, secondary OA usually occurs after injury or inflammation of a joint. Risk factors to the development of secondary OA are obesity and hip disorder such as osteonecrosis, development dysplasia of the hip, and hip fracture.[6]

The most common symptom of OA is pain in the hip or groin area especially during bearing activities.

Other indications for THA are:

- Rheumatoid arthritis, a chronic inflammatory disease that leads to joint pain, stiffness, and swelling
- Dysplasia of the hip in which patients are born with and develop an altered hip anatomy. It commonly leads to secondary osteoarthritis and eventually has to be treated with a THA at younger age. Due to the underdeveloped acetabulum and femur, THA is a very changeling procedure in these patients and often it requires revision surgery[7]

- Intraosseous or subchondral cysts are a fluid-filled space. They are frequently encountered in patients with dysplasia and OA. Cysts can lead to an erosion of the adjacent superolateral acetabulum that should be managed during THA[8]
- Avascular necrosis or osteonecrosis occurs when poor blood circulation causes osteocytes death and eventually hip joint collapse
- Ankylosing spondylitis is a chronic, inflammatory disease of the spine that can involve other joints.[9]

## 1.2 Total hip arthroplasty

The THA is an orthopedic procedure that involves the removal of the head of the femur, the creation of an medulluar canal to allow the insertion of the artificial femoral prosthesis as well as the reaming of the acetabulum in order to eliminate the cartilage and to insert the acetabular cup.[10] Figure 1.3 illustrates hip replacement surgery sequences and shows implant components.


*Figure 1.3 - Hip replacement surgery sequences. From left to right: preparation of bony structure, removing damaged bone and cartilage tissue; an example of an implant composed by an acetabular cup and an inner liner for the acetabular component and by a femoral stem and head for the femoral component; placement of acetabular and femoral prostheses to restore the joint.*[11]

To restore the joint many implant materials and fixation methods were investigated in the past. Before Charnley introduced the concept of low-friction arthroplasty in 1962,[12] endoprosthetic fixation into the medullary canal or in the acetabular cavity turned out to be difficult and failed in achieving long-term stability. Charnley's low-friction model was based on an immediate cement fixation of both acetabular cup and femoral stem. However, the belief that pelvic osteolysis of cemented arthroplasties was related to a biological reaction to the cement, led to the development and the spread of cementless hip systems.[13] moreover, the

cemented acetabular cups had a high loosening rate and, for this reason, the use of these implants has decreased, and they are usually adopted only in older patients, in patients with an avascular acetabulum due to previous irradiation or with complex revision acetabular reconstructions using antiprotrusio rings or cages.[14] On the contrary, the use of a cemented femoral component is still common.[15] Since the introduction of the cementless acetabular cup, different cup designs have been developed to provide stability. Achieving a solid primary fixation, in uncemented acetabular cups, is mandatory in order to ensure bone ingrowth and long-term stability. Threaded cups made by different materials with smooth surfaces were the first developed type, but the clinical results were disappointing. Later, threaded and expansion cups with grid-blasted surfaces were used but, long term failure rates were relatively high.[15,16] Press-fit hemispherical designs with porous and rough surfaces allow a good fixation and are currently the most frequently used cups. The porous surface can be obtained by sintering microsphere, beads, or powders on a substrate. Titanium has been used in porous coatings because of its biocompatibility and resistance to corrosion. Bone ingrowth into pores can occur if the primary stability, which is achieved using a meticulous surgical technique that provides compression by inserting a cup in an under-reamed cavity, is ensured.[17] Screw fixation may be required to achieve additional stability.[15] However, screw insertion may lead to injure neural or vascular intrapelvic structures and has to be avoided whenever possible.[18] The safest locations for screws fixation lie in the posterior superior and posterior inferior acetabular quadrants of a line from the anterior superior iliac spine through the center of the acetabulum to the posterior fovea and its bisector.[19,20] After the implantation of a press-fit acetabular cup, it will take approximately four to twelve weeks for osseointegration. Osseointegration can occur only if micromotions of the implant are minimized. Micromotion less than 28 μm does not inhibit bone ingrowth while the displacement of 150 μm or more stimulates fibrous tissue formation.[21] Relative motion between 40 μm and 150 μm leads to the formation of fibrous and bone tissue combination.[17]

### 1.2.1 Complications of total hip arthroplasty

Despite advances in technology and surgical techniques, multifactorial complications can occur after THA. Some of them, like thromboembolic disease and leg length discrepancy, can be treated with conservative methods, whereas others required a revision surgery.

*Fracture*

Periprosthetic fractures can occur either intraoperatively or in the postoperative period and can involve the femur or the acetabulum. The femoral ones are more common, and the

femoral neck is the most frequent site of the fracture. The risk factors are obesity, female gender, uncemented stem, osteopenia, and using excessive force during the implantation. The treatment depends on the site of fracture but is usually operative. Figure 1.4 depicts five common sites of femoral fracture.

*Figure 1.4 - Femoral fracture in different sites. A trochanteric fracture on the left, three different stem tip fractures in the middle and a distal fracture below the stem tip on the right.*[22]

Acetabulum fractures are less common and non-cemented components are the most inclined. Such a fracture can occur during acetabulum exposure, hip dislocation, reaming of the cavity, or impaction of the cup. The risk of fracture is increased using the elliptical component, under-reaming greater than 2 mm, and in the presence of abnormal bone (rheumatoid arthritis, Paget's disease, osteoporosis).[23,24] Late presentation of periprosthetic acetabulum fractures may occur as a result of trauma, migration of the socket and can be associated with infection. Acetabular fractures are more frequent in revision surgery than in primary THA. Additional screw fixation, placing a pelvic plate, or using a reconstruction cage can be used to manage and prevent this type of fracture.

*Dislocation*

Dislocation after hip replacement can require prolonged rehabilitation and, if it becomes recurrent, it can require a revision operation. Dislocations can be classified in early or late, and as single or recurrent. Late dislocation has usually a multifactorial etiology including component wear, pelvic osteolysis, and soft tissue laxity. Risk factors are implant component design and orientation, surgeon experience, the discrepancy in leg length, and abductor deficiency. The dislocation rate can be reduced by meticulous soft tissue repair.[25] Posterior lip augmentation devices can be used to treat patients unsuitable for revision THA. This C shape device is applied in the posterior lip of acetabulum with the use of five screws (Figure 1.5). It can lead to gross component malalignment and loosening.

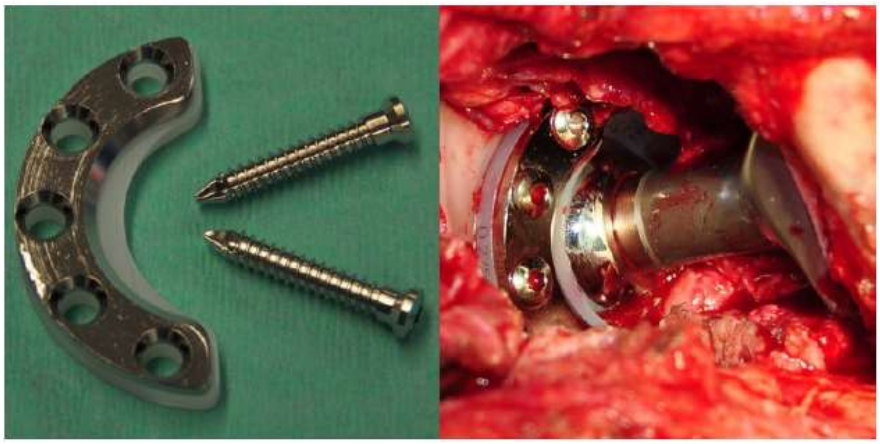

*Figure 1.5 - Posterior lip augmentation device.*[26]

*Aseptic loosening*

Aseptic loosening is the most common reason for revision of THA and the acetabular loosening is twice more likely than for the femoral stem.[27] It is the result of different complications like debris formation, prosthesis micromotion, and osteolysis. Malpositioning of the acetabular cup increases polyethylene wear and wear debris production.[28] Wear particles activate an immune response that can cause lysis of the bone that brings to aseptic loosening. Alternative bearing surfaces can be used to reduce debris generation. Treatment of aseptic loosening depends on the severity of the patient's symptoms and the complexity of osteolysis.[29]

## 1.3 Acetabular bone defects

Acetabular bone defects are characterized by bone loss caused by osteolysis. Osteolysis is a progressive and often asymptomatic phenomenon and can lead to implant migration and periprosthetic fracture. The management of acetabular bone loss is the most changeling aspect of revision surgery. Revision of THA occurs in only a minority of cases of total hip replacement but as younger patients are requiring hip replacement, the number of revision procedures will increase in the near future.[30]

The purpose of acetabular revision is to provide initial and stable fixation of the cup, to restore the center of rotation and to recover bone stock if possible. A meticulous preoperative characterization is necessary to plan a suitable treatment. Numerous classification schemes have been proposed in order to predict bone loss and plan the most appropriate treatment. These classifications are also a useful method to compare the outcomes of different treatments.

### 1.3.1 Classification systems

*AAOS classification*

The American Academy of Orthopedic Surgeons (AAOS) classification was the first classification system developed by D'Antonio et al. for acetabular defects in 1989.[31] It is a qualitative system in which the defects are classified in two basic categories: segmental (type I) and cavitary (type II). Segmental or rim defects are complete bone loss in the supportive hemisphere of the acetabulum. Cavitary deficiencies consist of a volumetric bone loss of the acetabulum cavity but with an intact rim. Both deficiencies can be peripheral or central and may appear isolated or can coexist (type III). In the presence of a pelvic discontinuity, the defect is classified as type IV and with an arthrodesis as type V. AAOS classification system does not provide any guidelines for the reconstruction options. Figure 1.6 reproduces the different AAOS defect types.

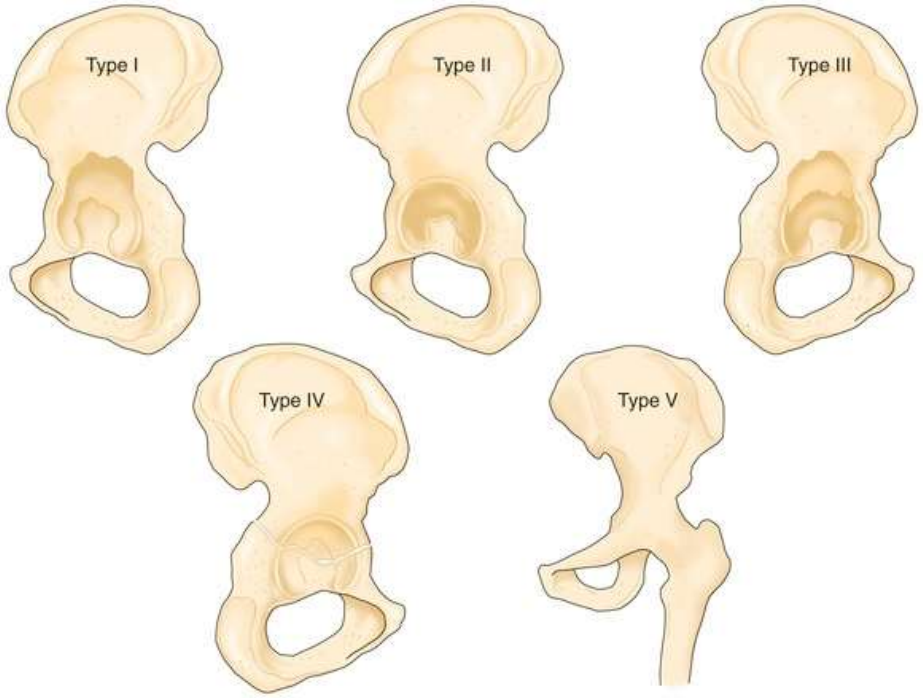


*Figure 1.6 - AAOS classification of acetabular bone defects. From left to right: type I - segmental deficiency, type II - cavitary deficiency, type III - combined deficiency, type IV – pelvic discontinuity, type V – arthrodesis.*[32]

*Paprosky classification*

The Paprosky system is based on the integrity of the acetabular supportive structures and on the amount of cup migration.[33] The main supportive structures are the medial wall, the superior dome as well as the anterior and posterior columns. The evaluation is based on preoperative radiographs. The defects are divided into three types characterized by an increase of bone loss and, for every type, advice for the surgical reconstruction is given. Types 2 and 3 are divided into subtypes. Furthermore, for each defect type different methods of reconstruction are proposed.

In type 1 defect, the rim is intact, and the acetabulum shows minimal deformity. No migration of the component is displayed on the preoperative radiograph and the teardrop is present. Bone lysis is restricted around cement anchor holes.

In type 2, the acetabulum hemisphere is partially distorted, but the anterior and posterior columns are intact and supportive. The migration of the component is less than 2 cm. Type 2 defects are further divided into three subtypes according to the site of defect and direction of hip center migration. In type 2A defects, the acetabulum displayed an oval enlargement with a superior bone loss. The superior rim remains intact. The radiograph shows a superior migration of the cup. Type 2B defects are characterized by the absence of the superior rim and the distortion of the dome. The deficient superior dome allows a superior-lateral migration of the component. In type 2C defects, the medial wall and the teardrop are absent, and the hip center migrates medially.

Type 3 defects show severe osteolysis with the destruction of the superior rim and non-supportive columns. These defects could be combined with pelvic discontinuity and lead to a component migration greater than 2 cm. Type 3 defects are divided into two subtypes. In type 3A defects, there is a moderate destruction of the teardrop and moderate lysis of the ischium. Kohler's line remains intact avoiding medial migration of the cup. The component has a superolateral migration. The acetabular rim is absent from 10 o'clock to 2 o'clock position with a lack of 30% to 60% of bone stock. Type 3B defects are the most severe and are characterized by the complete destruction of all supportive structures that leads to a superomedial migration of the hip joint center. The acetabular rim is absent from 9 o'clock to 3 o'clock position with destruction greater than 60% of bone stock. Figure 1.7 shows the different types of acetabular defects in Paprosky classification.

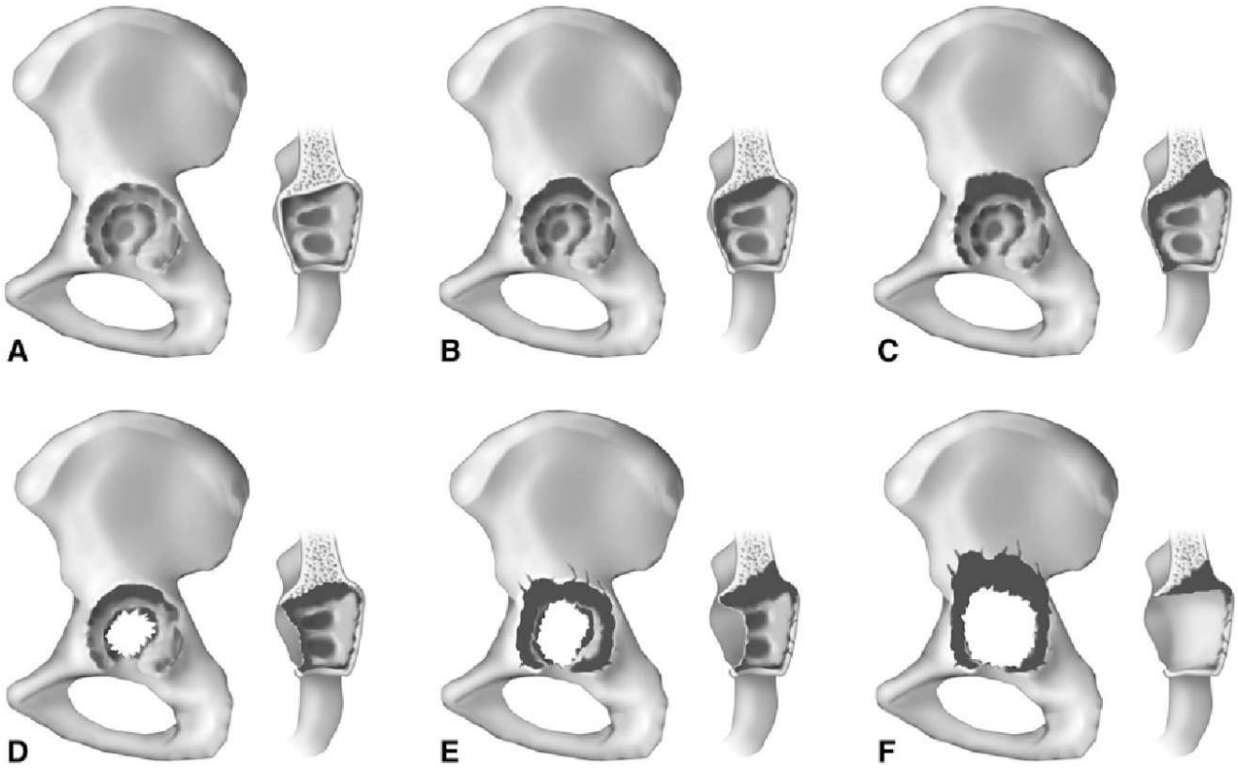


*Figure 1.7 - Paprosky classification of acetabular bone defects. A) Type 1, B) Type 2A, C) Type 2B, D) Type 2C, E) Type 3A, and F) Type 3B.* [34]

*Other classifications*

Other classification systems were developed after AAOS and Paprosky classifications. Two of them are Gross classification[35] and Parry classification[36].

The first one classifies bone loss and relates it to surgical treatment needed. It divides acetabular defect into 5 types: in type I there isn't a substantial bony loss, in type II there is a contained bone loss with intact rim and columns, in type III the bone loss is uncontained but less than 50% of the acetabulum is involved, type IV is analogous to type III but the loss of bone stock is greater than 50%, and in type V there is a pelvic discontinuity with uncontained bone loss (Figure 1.8).[37]

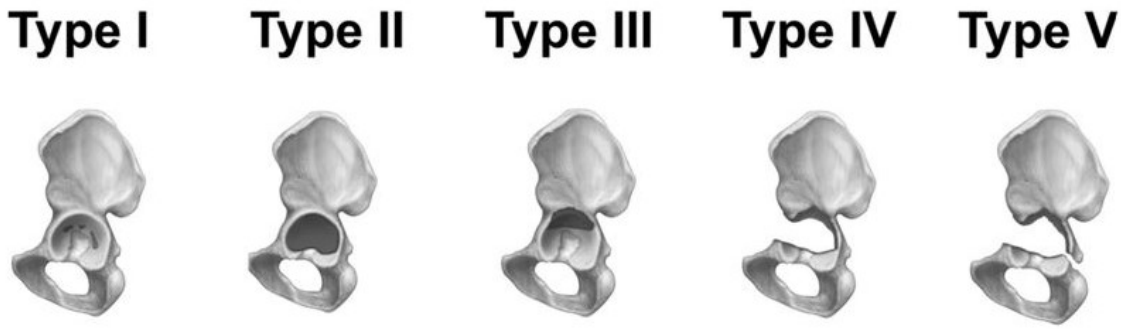


*Figure 1.8 - Gross classification of acetabular bone defects.*[38]

Parry classification grades the defects primarily as contained or uncontained and then suggests a reconstruction technique. Acetabular defects are divided into three categories: A)

contained defects with minimal bone stock loss, B) contained defects with large bone stock loss and C) uncontained defects.[36]

### 1.3.2 Validation of the classification methods

A high degree of reliability and validity is a crucial requirement of a classification system. Reliability refers to the consistency of a classification among users. This is divided into intraobserver reliability considering the agreement of the same person in different moments and in interobserver reliability considering the agreement among different subjects. Validity refers to how closely the preoperative classification predicts the actual defects. The reliability of all classification systems has been assessed in different studies.[34,36,39,40] Intraobserver reliability was poor to moderate and interobserver reliability was poor for all the previous classification methods.[39] An improvement of interobserver reliability was found after teaching sections of the Paprosky system. Good validity of Paprosky system was found comparing classified defects with the actual ones.[40]

Acetabular defects are mainly classified as inspecting preoperative radiographs. In the radiographic examination, some structures can be obscured and orthopedic surgeons can underestimate pelvic osteolysis.[41] An accurate method for detecting and quantifying pelvic lysis is computed tomography (CT). The quality of the images has been improved by the use of metal artifact suppression protocol.[42] Furthermore, the classification becomes usually more difficult without the native pelvic anatomy for comparison, and in this case, the application of a statistical shape model is a promising option to recreate the native pelvic based on a defect pelvis.[43] However, CT uses a higher dose of radiations for imaging and it should be used only when necessary for preoperative planning.

### 1.3.3 Reconstruction methods

Different treatment options are available for revision THA depending mainly on the degree of bone stock loss.

*Cementless hemispherical cup*

Porous coated cementless hemispherical cups can be used in most acetabular revision procedures in which contact between the implant and host bone is at least 50%.[44] Porous coating and porous metal improve initial stability required for bone ingrowth. Screws are often used for a supplemental fixation.[17] Impaction grafting can be used to fill contained defects. Morcellised allografts can be inserted into the defects using acetabular reamer in reverse.[45] In cases of major bone loss, the jumbo cup (>62 mm for women and >66 mm for men) can restore the hip joint center of rotation, thus reducing the need for bone grafting.[46]

The main disadvantages of jumbo cups are that they may not restore bone stock, has a high rate of dislocations, and compromised implant stability due to the excessive reaming required. Like in the primary THA, the primary stability for an uncemented cup is achieved using a cup 1-2 mm larger than the reamed cavity.

*Structural grafting*

Structural graft can be used when the remaining supportive acetabular structures cannot achieve a reliable fixation and primary stability of the cup. Bone grafting can be made with autogenous, allogenous, or artificial bone material. Autografts are the most suitable grafts due to their histocompatibility, osteoconductivity, and the lack of viral transmission risks. However, autograft is usually not available in hip revision and thus allograft is widely used. Three different types of allograft are available: fresh frozen, irradiated, and freeze-dried bone. Allografts have good availability, but they can cause immune response and risk of infection (fresh frozen) or can have reduced mechanical and osteoinductive properties (freeze-dried). Irradiated allografts show a high fracture risk. Ceramics or bioglass are used as artificial bone material.[47] In hip revision, both bulk allografts and morselized allografts are used (Figure 1.9). Bulk grafts are used in case of massive bone loss and have the potential advantage of inducing the restoration of bone stock and immediate structural support, but graft resorption often occurs in bulk allografts. Cancellous allografts have a quicker osteointegration but do not provide structural stability. Structural graft achieves better results when it supports less than 50% of the acetabular implant. Otherwise, a reinforcement ring or cage should be used.

*Figure 1.9 - Bone allograft. Cancellous bone chips (left) and volume-rendered CT scan shows a femoral condyle allograft bone that will be cut into "figure-7" shapes (right).*[48]

*Reinforcement rings and reconstruction cages*

Reinforcement devices that span ilium to ischium can support massive structural allografts. The roof reinforcement ring preserves the superior acetabular dome, while the antiprotrusio

cage extends from the ilium to the ischium providing a larger contact area between the bone host and the implant. A liner can be cemented into the cage in an appropriate position and inclination. Cage and ring enable the restoration of the hip joint center and support the remodeling of the graft as well as the integration into the host bone by a smooth transfer of the load. There is a high risk of cage fracture and loosening, however, an uncemented cup can be used in the following revision if the graft is incorporated.[18] Due to the high rate of complications, the use of reinforcement devices has decreased and the interest in porous metal components has increased. Figure 1.10 illustrates different types of reinforcement devices.

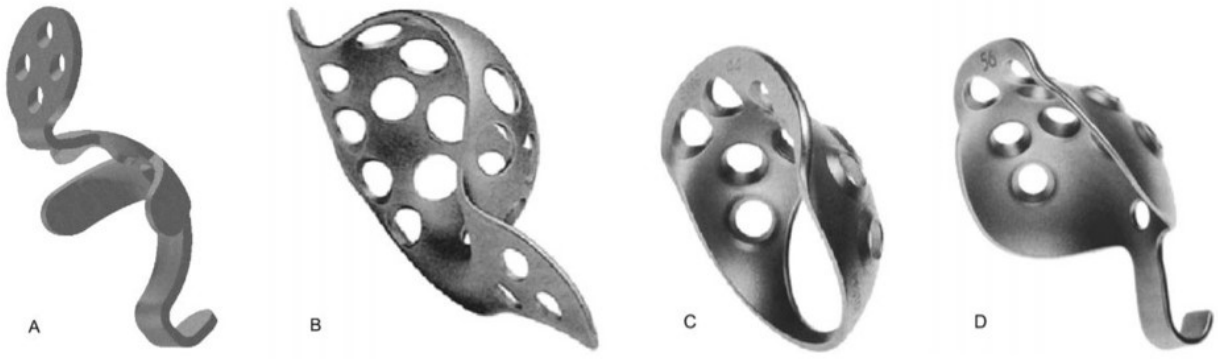


*Figure 1.10 - Acetabular reinforcement devices. A) Kerboull-type device, B) Burch-Schneider antiprotrusio cage, C) Mueller support ring, D) Ganz reinforcement ring.*[49]

*Trabecular metal augments and shell*

Trabecular Metal™ (TM, Zimmer Inc., Warsaw, IN, USA) systems are designed to allow maximum biological fixation. TM is an 80% tantalum alloy with a suitable elastic modulus and a high friction coefficient. TM has a microscopic structure, shown in Figure 1.11, similar to that of a cancellous bone that promotes bony ingrowth for biological fixation.[50]

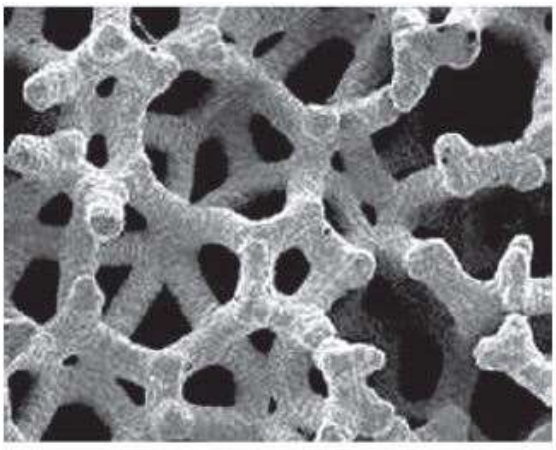

*Figure 1.11 - Electron microscope view shows TM microscopic structure.*[48]

In the presence of a segmental bone loss, a tantalum augment can be added to TM acetabular component. Augments replace the need for structural allograft providing structural support for the acetabular cup. An example of a trabecular metal cup and augment is shown in Figure

1.12. For the insertion, after the preparation of the acetabular cavity with a reamer, the optimal position for the cup and the augments is determined using trial devices.[51] Definite augments are then impacted and secure with screws into the acetabulum. The acetabular component is press-fitted into the cavity after a polymethylmethacrylate cement layer has been placed between the augments and the cup.[52] Potential problems are the generation of debris at acetabulum augments interface and the lack of bone stock restoration for the following revisions.

*Figure 1.12 - A trabecular metal acetabular component and a trabecular metal augment.*[53]

*Cup-cage reconstruction*

In order to avoid structural allografts in the presence of severe defects, orthopaedic surgeons can use morselized bone graft with a cup-cage reconstruction. A porous metal acetabular shell is used to achieve a biological fixation while a cage spanning ilium to ischium is placed on the top of the cup to ensure the initial mechanical stability. A polyethylene liner can then be added.[54] A model of implantation and of implant components are represented in Figure 1.13.

*Figure 1.13 - Cup-cage implant model (left), cup-cage components (right).*[55]

*Custom-made acetabular component*

An alternative method to achieve biological fixation when severe acetabular defects are present is the use of custom-made acetabular cups (Figure 1.14). This device spans ilium, ischium, and pubis with three rigid flanges, in order to provide areas of contact with host bone to achieve initial stability through screw fixation. A scan of the pelvis is obtained using a thin-cut CT data and models of the hemipelvis as well as a prototype of the implant is created using a metal subtraction software. After the approval of the initial design, the final implant is produced. The porous coating of the device potentially allows bone ingrowth. The main disadvantages of this treatment are the complexity of pre-operative planning, the surgery delay and the expensive cost of the entire process.[56]

*Figure 1.14 – Custom made triflanged acetabular cup from the front (left) and from back (right) view. The backside has a porous coating for long-term biologic fixation.*[57]

## 1.4 Measurement of acetabular cup fixation

The primary stability of acetabular cups is of paramount priority for the long-term success of cementless cups. High primary stability allows bony ingrowth providing a good secondary stability of the implant. Initial stability can be defined as the lack of relative micromotion between the cup and the bone in the first 90 days after hip replacement.[58] Experimental measurement of acetabular fixation can be performed with different tests. The tests can be conducted using human pelvic specimens, bovine bone specimens, or artificial bone materials.[59] The use of cadaveric specimens may lead to a more representative intraoperative situation but have many limitations including small sample availability, high cost, high inter-specimen variability, high rate of specimens decay, and ethical problems. The use of bovine specimens can overcome the first two disadvantages of cadaveric specimens but doesn't solve bone density variability. Synthetic polymer foam such as polyimide (PMI), polyvinylchloride (PVC), or polyurethane (PU) can be used in the form of anatomical bone shape or as test blocks to simulate cancellous bone. PU foam is widely used in biomechanical tests.[60,61,62,63,64]

It has a closed microscopic structure, shown in Figure 1.15, that is quite different from the open porosity of trabecular bone, but it is ideal for comparative testing of medical implants.

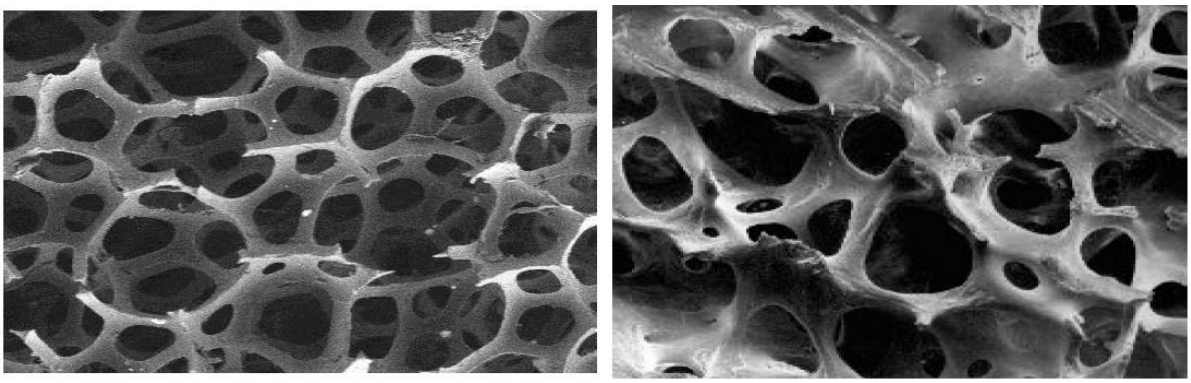

*Figure 1.15 - Microscopic structure of PU foam (left) and cancellous bone (right).*[65]

Like trabecular bone, PU foam is not resistant to tension, or shear and the compressive stress-strain curve shows three regions (Figure 1.16). The first region is characterized by a linear elastic behavior controlled by cell wall bending. The plateau region is correlated to cells collapse due to elastic buckling and brittle crushing. Finally, there is the densification region with a rapid increase in stress.

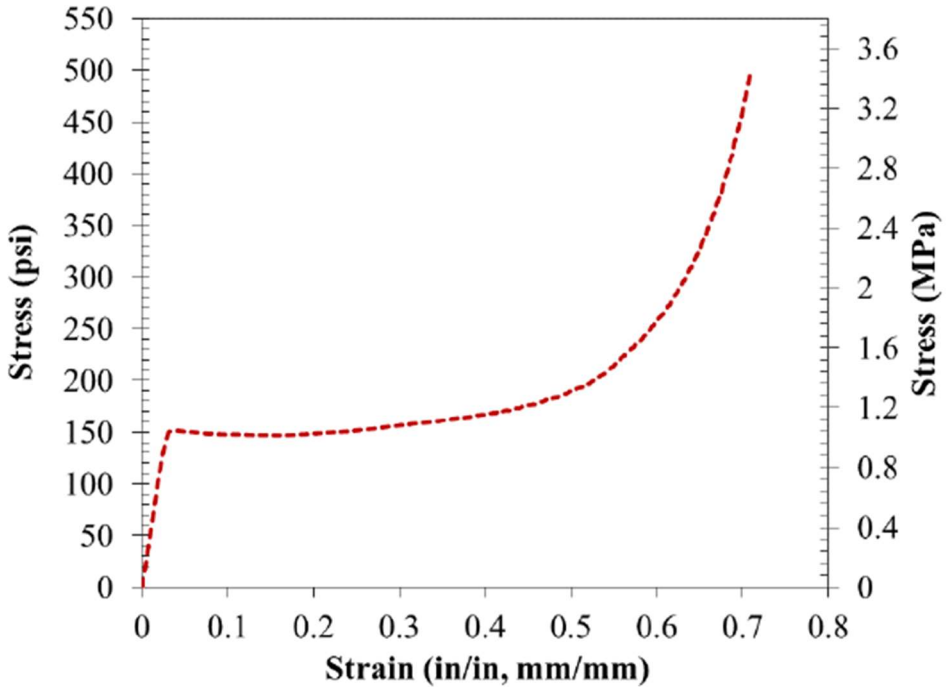


*Figure 1.16 - Typical compressive stress-strain curve for a PU foam.*[66]

The main test methods used in literature to assess primary stability are pull-out test, push-out test, lever-out test, and torque test. To conduct these tests, the cup is first pressed into the block cavity using a load or a displacement control protocol[16,67] or replicating the effect of hammer blows during the impact of the cup in the cavity.[68,69]

Usually, a rod inserted in the cup pole is loaded in the longitudinal direction for the pull-out and the push-out test[70], in perpendicular direction for the lever-out test[71] or with a rotational speed for torque test.[72] During the tests, the forces and moments needed to extract the cup are recorded. Another key parameter for initial stability is interface stiffness between the cup surface and the block, defined as the slope in the linear portion of the force-displacement curve after the first cup motion, during the extraction. Figure 1.17 depicts schematically three different test methods.

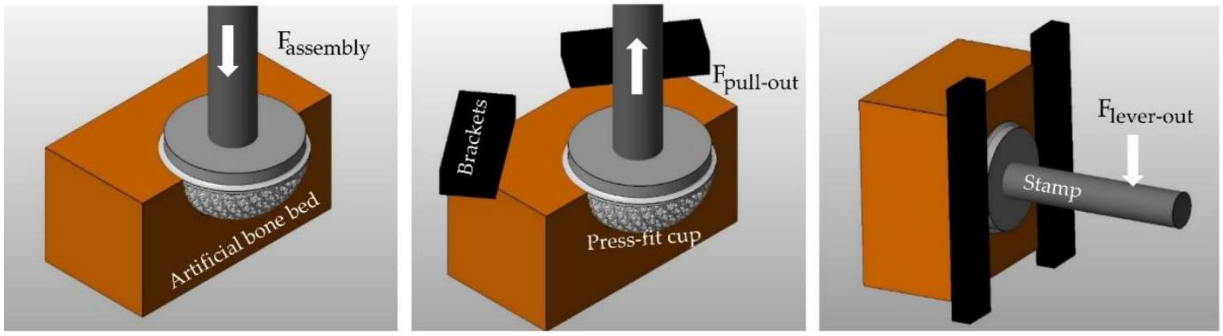


*Figure 1.17 - Schematic representation of the experimental test environment. From left to right: insertion of the cup, pull-out test, and lever-out test, conducted by applying a pulling or a levering force respectively and recording the applied load until failure of implant anchorage.*[73]

Lever-out tests were carried out in this Thesis in order to investigate the primary stability of two acetabular cups using PU-foam blocks. The tests were performed under displacement-control conditions using a static universal testing machine (Zwick/Roell Z050, Zwick GmbH & Co. KG, Ulm, Germany).

## 1.5 FE model

Besides in vitro testing, another approach often used to assess the primary stability of acetabular shells is computational modelling. The finite element method is a powerful numerically technique that allow the study of complex physical phenomena. To investigate biological problems, numerical simulations are usually performed in combination with experimental tests that provide the boundary conditions and the data for the validation of the FE model. This combined in vitro – in silico approach grants a wide overview in various scenarios reducing the high cost related to experimental tests.[74]

Nowdays, different softwares are available in order to create FE models. Abaqus FE software (v 6.12 Dassault Systèmes, Simulia, Providence, RI, USA) was used in this Thesis. The FE analysis consists of three stages: pre-pocessing (Abaqus/CAE), processing (Abaqus Standard) and post-processing (Abaqus Viewer). In the pre-processing part, the model is generated. The geometries of the parts are created and assembled and the materials properties are specified and assigned to the parts. Then the interaction between the parts and the steps needed to

perform the simulation are pointed out and the loads and the boundary conditions are defined. Moreover, the parts are discretized into finite elements by meshing their geometries. This is a crucial point of the numerical simulation as the mesh density and the type of elements used to mesh the part can deeply affect the accuracy of the results.[75] A convergence analysis should be carried out in order to evaluate the best mesh density for the model. The density of the mesh can be managed using a local seed. The local seed can be managed increasing the number of elements along a direction (bias seeding) or making a partition of the part (mesh refinement). Therefore, the simulation can be runned and the model, defined in the pre-proccesing stage, can be solved (processing stage). The results are then displayable in the post-processing stage using Abaqus Viewer. Here the results can be visualized and manipulated to obtained x-y plots as well as images and videos of the simulation.

## 1.6 Aims and motivations

Assessing the fixation of acetabular implants in the presence of defects has been a widely analyzed and debated problem in the last decade, by means of both experimental tests and numerical simulations, using different defects models. Gorianov et al. examined the relationship between the outer surface characteristics of the cups and their stability, using two revision shells inserted in Sawbones blocks. The blocks replicated different segmental defects, defined by an angle $\alpha$.[62] After the insertion, a torsional test was carried out to evaluate the initial stability of the cups. Crosnier et al. investigated the influence of the bone density and acetabular geometry on the stability of the implant. They inserted a revision uncemented cup in two Sawbones blocks of different densities, which replicate two acetabular geometries (an intact and a defect cavity).[76] To define the geometry of the defect they used a two point-pinching block (Jin's defect).[77] Recently, Schulze et al. tested a primary cup in the presence of different acetabular defects using PMI foam blocks.[78] Their study highlighted how the stability of a primary cup was compromised by the presence of large defect. The aims of this Thesis was to investigate the primary stability of acetabular cups under consideration of different acetabular defects. In the experimental part, a revision and a primary acetabular cups were compared in order to consider the influence of the type of implant on the primary stability of the cup for the different acetabular geometries. For the numerical model, only a primary cup was used investigating its stability in different densities of the foam block.

# 2. Materials and methods

## 2.1 Experimental testing

### 2.1.1 Acetabular cups

Two different uncemented acetabular cups were tested in experimental cup-block models to establish their primary stability in three different Sawbones® (Pacific Research Laboratories, Inc., Vashon, USA) blocks with a density of 0.32 g/cm$^3$ and various defect sizes.
Both primary and revision cups with an outer diameter of 56 mm were used (Figure 2.1).

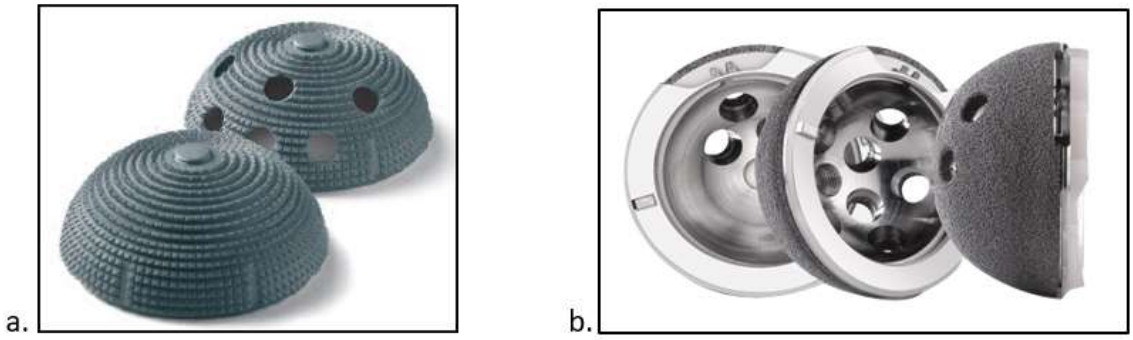


*Figure 2.1 - a. Allofit® primary cups (Zimmer, Warsaw, IN, USA)[79], b. Trabecular Metal™ revision shell (Zimmer, Warsaw, IN, USA).*[80]

The Allofit® cups have a hemispherical shape with a slightly flattened dome. Its macrostructured surface, made up of fine barb-shaped teeth, increases the surface contact with bone, improving implant fixation and provides a more stable biological fixation of the implant.[51,81,82] Long-term anchoring through osseointegration is ensured using a proven material for the cup, the titanium-wrought alloy Protasul®-Ti with a rough-blasted surface. The Allofit® Alloclassic® cup without screw holes was used in all the experimental tests.
The Trabecular Metal™ revision shell maximizes initial and long-term stability with an elliptical geometry, that brings to a 2 mm interference fit at the periphery. Implant stability is also increased thanks to the great porosity of TM that together to its low stiffness allows bone ingrowth.
The parameters of the two cups are summarized in the table below.

*Table 2.1 - Allofit® Alloclassic® cup and Trabecular Metal™ revision shell features*

| | Cup type | Size (mm) | Nominal diameter (mm) | Outer surface | Surface structure |
|---|---|---|---|---|---|
| **Allofit®** | Primary | 54 | 56 | rough blasted barb-shaped teeth | hemispherical with flattened dome |
| **Trabecular metal™** | Revision | 54 | 56 | high porosity TM | elliptical |

### 2.1.2 Defect models

The primary stability of the cups previously described was investigated for a moderate and a large defect as well as for the intact cavity. The defect size of the bone models was defined by two angles (angle α and angle β) that described two directions of bone loss. Angle α referred to a superior rim loss, while angle β referred to a medio-lateral wall absence, related to the center of rotation of the reamed acetabular cavity (Figure 2.2).[78] Two different defect sizes were considered: the moderate defect had α = 90° and β = 45° (90/45 defect), the large defect had α = 120° and β = 45° (120/45 defect). The moderate defect corresponds to a critical uncovered superior portion of about 50% above the cup.[41,83] The largest defect (120/45) was chosen to underline the different behavior of the primary cup and the revision cup in the presence of large acetabular defects. The hemispherical cavities and the defects were milled in Sawbones® blocks with a density of 20 pcf, using a CNC-machine, in order to obtain reproducible conditions. All the cavities were 2 mm under-reamed if compared to the cup nominal outer diameters to achieve the initial fixation.

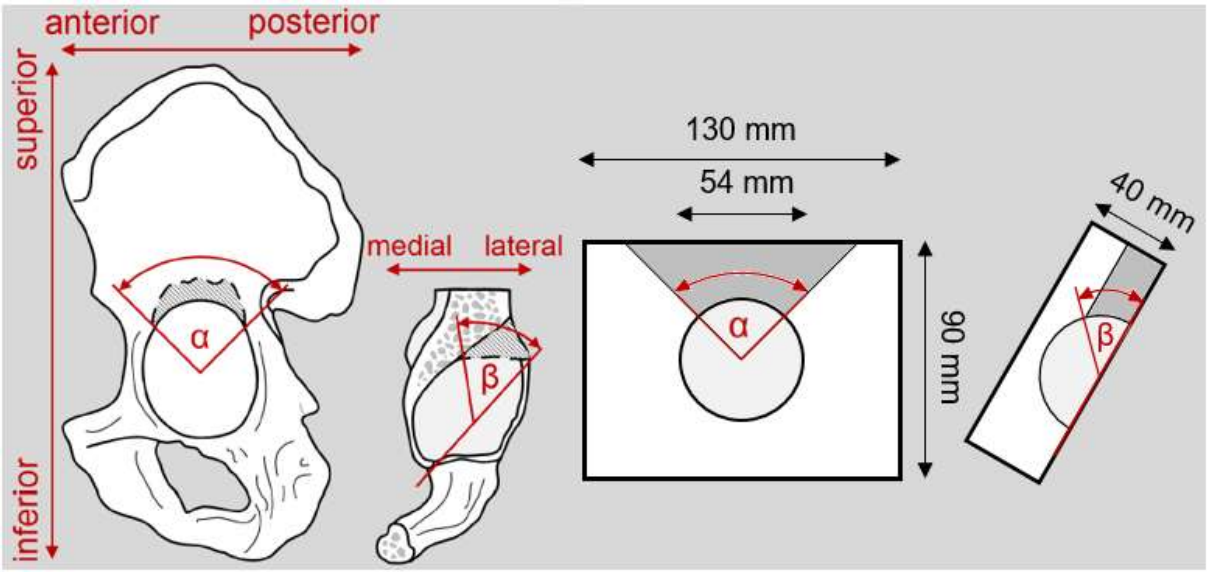


*Figure 2.2 – Schematic view of the pelvic defect (left) and defect milled in the experimental block models (right).[78] Angle α and angle β describe superior rim loss and medio-lateral wall damage respectively.*

The actual diameters of the cups and the cavities of the blocks were measured before the experimental tests were performed. The measurements were conducted in another laboratory using a ZEISS DuraMax (Carl Zeiss Industrielle Messtechnik GmbH, Oberkochen, Germany) with the ZEISS Calypso software.

Lever-out tests were carried out to assess and to compare the primary stability of the acetabular cups in the different Sawbones® blocks.

For each cup, block type, and test method, five replicas were executed. At the end of each test, the cups were cleaned with brushes and were checked to ensure that no damages had occurred during the test.

### 2.1.3 Press-fit test setup

Two cups of each type were used to perform all the experimental tests. Each PU-foam block was randomly assigned to a cup. The insertion and the extraction of the cup was carried out with a static universal testing machine (Zwick/Roell Z050, Zwick GmbH & Co. KG, Ulm, Germany) using a shaft screwed into the threaded pole of the implant. The shaft was axially connected to the testing machine, whereas the Sawbones® blocks were mounted on a thrust ball bearing to prevent transverse loads during the cups' insertion (Figure 2.3).[78] Before the push-in process, the foam blocks were manually aligned to the cups.

*Figure 2.3 – Press-fit test setup. Insertion of the TM cup in the block with the intact cavity. From the upper part of the figure: loading cell, connection adaptor, shaft, cup, artificial bone block, and shear force bearing.*

*Preliminary tests*

Preliminary tests for both the cups were performed to establish the seating position and for each combination of cup and PU foam block, three replicas were carried out. The cups were pressed into the cavities under load-controlled conditions at a crosshead velocity of 20 mm/min. The insertion of the cups stopped as the set load was reached. The ultimate loads were 10 kN (intact cavity), 9 kN (90/45 defect), and 7 kN (120/45 defect). The displacement and the force were recorded during the insertion using TestXpert II (Zwick GmbH & Co. KG, Ulm, Germany). Subsequently, the data were imported in MATLAB 2017b (MathWorks Inc., Natick, Massachusetts, USA) in order to determine the seating position of the cups for the main test according to the method of Small et al..[64] Since the last region of the force-displacement curve is nearly linear the best fitting line was calculated, computing a linear least squares fitting, and then shifted by 0.1 mm. The force value, corresponding to the point of intersection between the force-displacement curve and the shifted line, was defined as the seating force (Figure 2.4). The seating position was therefore defined knowing the displacement of the cup corresponding to the seating force and its initial position.

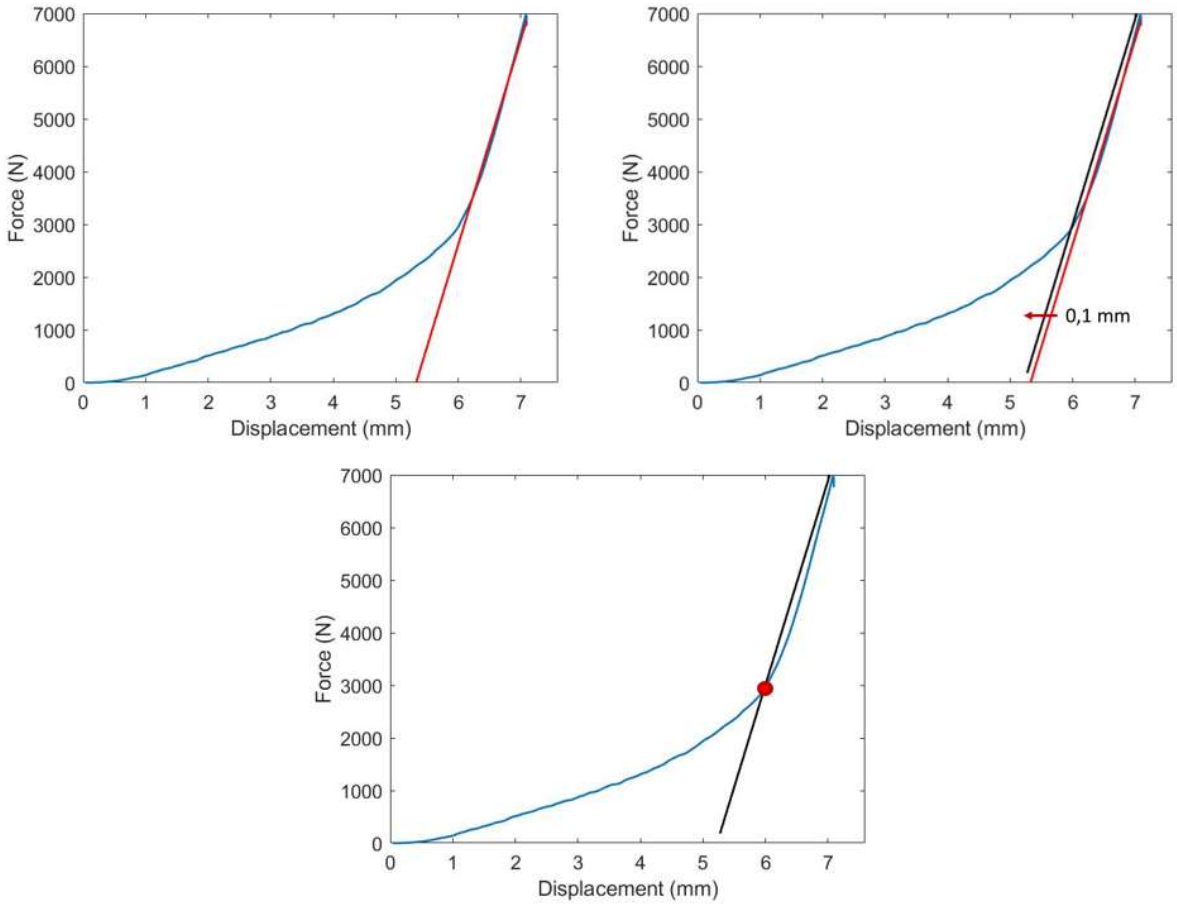


*Figure 2.4 - Determination of the seating force: a. linear regression of the last linear elastic region of the force-displacement curve; b. 0.1 mm shifting of the regression curve; c. detection of the seating force highlighted by the red dot.*

*Push-in test*

The push-in and lever-out tests were performed with the same static universal testing machine that was used for the preliminary tests and the data were then elaborated in MATLAB 2017b. The implants were pressed into the cavities at a crosshead velocity of 20 mm/min under displacement-controlled condition until the seating position determined in the preliminary tests was reached. The push-in force was recorded, using TestXpert II, during the insertion.

### 2.1.4 Lever-out test setup

The cup-block assemblies were vertically fixed, and the acetabular cups were levered-out, under displacement control conditions, at a crosshead velocity of 20 mm/min. The lever-out shaft was moved in the direction of the intact rim, reproducing a superior dislocation (Figure 2.5). The reaction force was recorded until the cups were dislodged from the cavities.

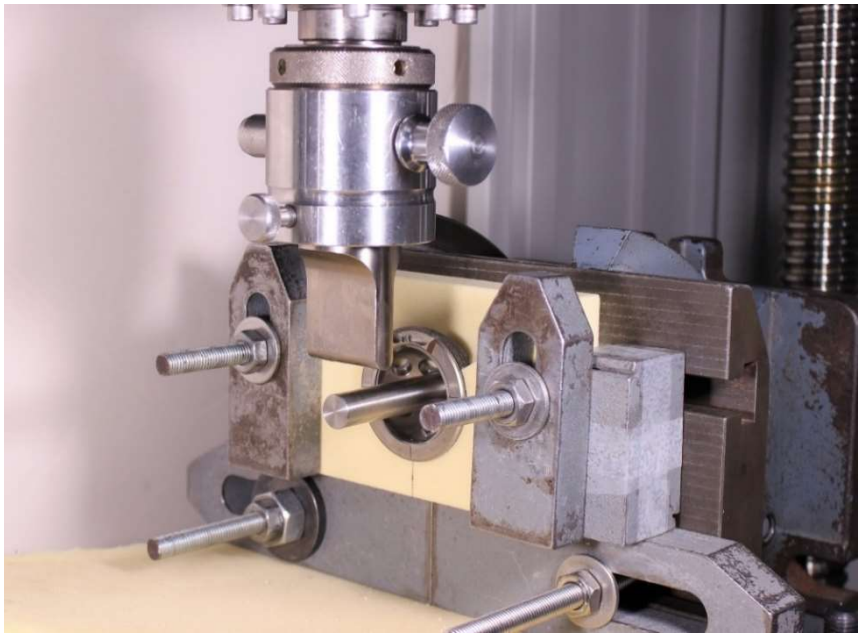

*Figure 2.5 - Lever-out test set up. Lever-out test conducted for the TM cup in the PU foam block with the 120/45 defect.*

The vertical orientation of the cup-block assemblies led to an additional force caused by the shaft deadweight ($F_d$) (Figure 2.6). The lever-out moment ($M_{lever\text{-}out}$) was calculated in MATLAB as the sum of the moment due to the lever-out force ($F_{lever\text{-}out}$) and of the deadweight moment ($M_d$):

$$M_{lever-out} = F_{lever-out} \cdot l_{lever-out} + M_d \quad (1)$$

Where $l_{lever\text{-}out}$ was the lever-out arm, defined as the distance between the point of the applied displacement on the shaft and the ideal acetabular center of rotation, and $M_d$:

$$M_d = m_{shaft} \cdot g \cdot l_{shaft} = F_d \cdot l_{shaft} \quad (2)$$

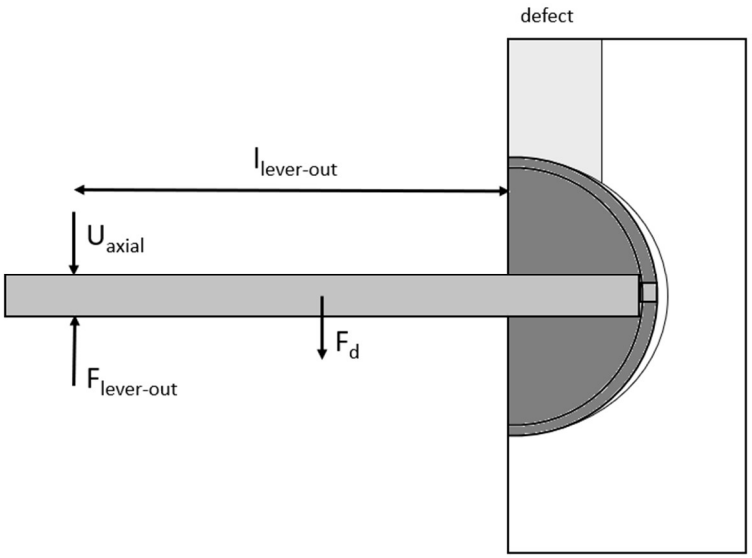


*Figure 2.6 - Schematic view of the lever-out test. $U_{axial}$ is the axial displacement along the vertical direction, $F_{lever\text{-}out}$ is the reaction force to $U_{axial}$, $F_d$ is the deadweight of the shaft, and $l_{lever\text{-}out}$ is the length of the lever-out arm. The light gray part, underlined in the PU-foam block, represents the medio-lateral defect.*

The work needed to lever-out the cup was also recorded and used to compare the cup lever-out process on the basis of an additional parameter.

The interface stiffness between the acetabular cup and the PU foam was considered as another primary stability parameter. It was defined as the maximum linear slope in the force-displacement curve until the maximum force was reached (Figure 2.7).

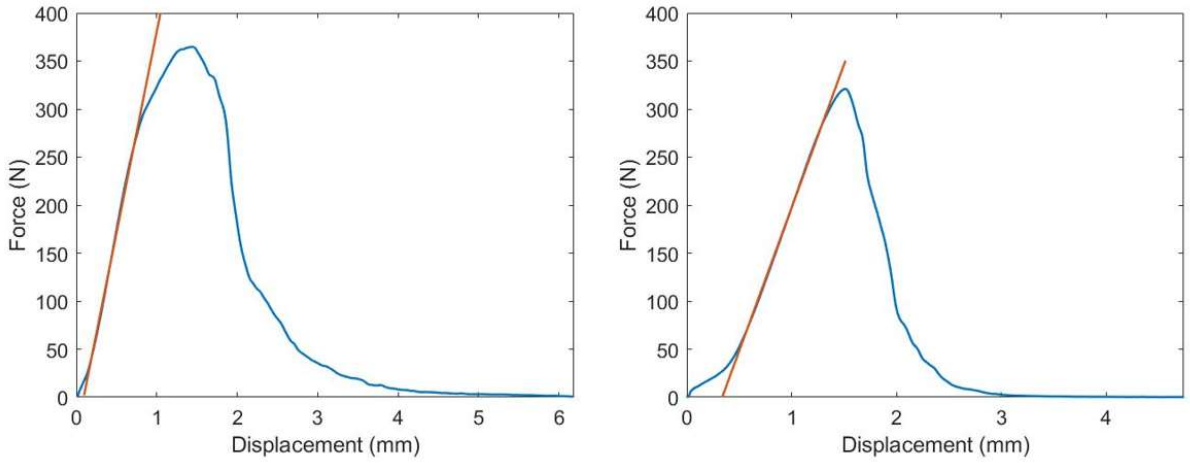


*Figure 2.7 - Force-displacement curve during lever-out (blue). The red curve represents the computed interface stiffness. On the left: the Allofit cup in an intact cavity block; on the right: the TM™ cup in an intact cavity block.*

### 2.1.5 Statistical analysis

All the parameters were compared using the mean values averaged over the five replicas and the standard deviations.

A statistical analysis was executed using IBM SPSS Statistics 25.0 (IBM Corp. Released 2017. IBM SPSS Statistics for Windows, Version 25.0. Armonk, NY: IBM Corp.). A

Shapiro-Wilk test was carried out to verify the normal distribution of the data. Then, as the data of the push-in force, the lever-out moment, and the interface stiffness violated the assumption of homogeneity of variance needed to perform Classic ANOVA, a Welch-ANOVA analysis was implemented. A One-Way ANOVA analysis was performed instead on the lever-out work. Games-Howell and Bonferroni post hoc tests were carried out after the Welch-ANOVA and the One-Way ANOVA, respectively, to obtain intergroup comparisons. The aim of these tests was to discover whether the presence and the size of the defect as well as the type of implant (primary or revision cup), determine a significant difference in the parameters used to assess primary stability.

## 2.2 Numerical simulation

The numerical simulations were performed using Abaqus/CAE FE software (v 6.12 Dassault Systèmes, Simulia, Providence, RI, USA). For the numerical simulation, two FE models should have deployed for the two Zimmer cups to compare the experimental results of the push-in and lever-out tests in the different PU foam blocks. However, CAD files of the two cups were not available. Moreover, the reconstruction of the geometry of the outer surfaces the Allofit cup would have led to an impossible meshing process, due to the sharp teeth presented on the surface.

In order to evaluate the influence of the defects in primary stability the CAD file of a different acetabular cup, the SeleXys PC® (Mathys AG Bettlach, Bettlach, Switzerland), was used. The SeleXys PC® is a primary modular cup with an elliptical shell with a 2 mm oversizing included at the equator and a flattened pole area. The cup used for the numerical simulation had a maximum outer diameter of 54 mm and a total height of 28 mm.

Previous experimental tests had been performed with the SeleXys PC® cup and Sawbones® blocks with two different densities (15 pcf and 30 pcf). To validate the FE model with the experimental result the same intact PU foam blocks were used in the simulation.

The defect geometries were reconstructed in the CAD file of the PU foam blocks to perform the simulations in the presence of the defects. Therefore, the results of the cup-block FE models with the two defects were compared to the ones of the intact model to establish the influence of defects in primary stability. The parameters influencing the primary stability, considered for the comparison, were the maximum force needed to insert the cup into the cavity of the blocks (Push-in force), the maximum momentum recorded during the lever-out simulation (Lever-out moment) and the interface stiffness between the cup outer surface and the cavity surface of the Sawbones® blocks. Other important parameters that were computed

during the simulations were the contact pressure and the contact area between the cup and the cavity of the blocks. The contact area is indeed considered a crucial factor influencing cups primary stability.[59,84,85,86]

### 2.2.1 Description of geometry

*Blocks' geometries*

The geometry of the PU foam blocks was reconstructed in SolidWorks 2015 (Dassault Systèmes, Vélizy-Villacoublay, France) and exported in Abaqus/CAE 6.12 (Figure 2.8).

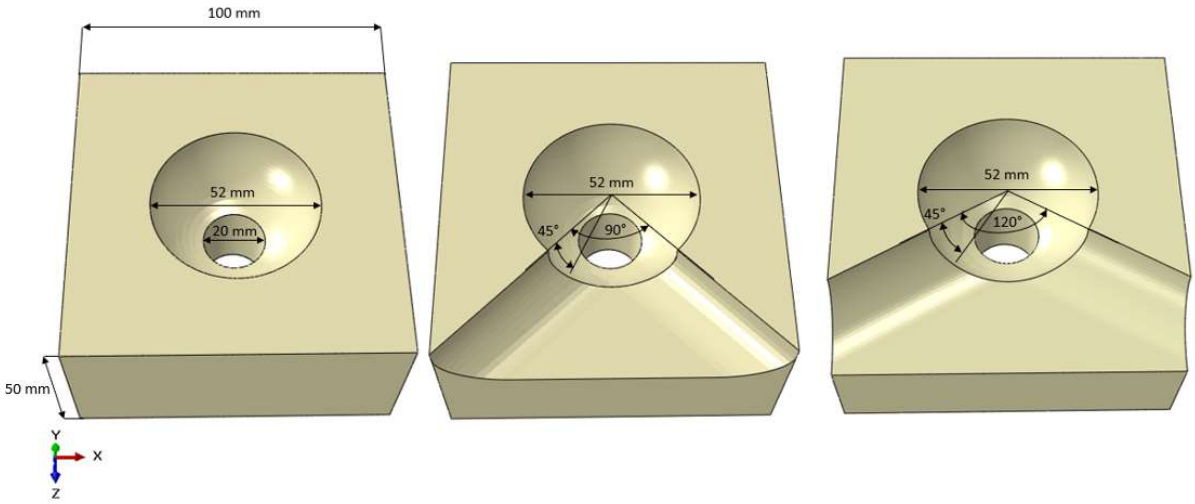


*Figure 2.8 - PU-foam blocks geometries. From left to right: intact model, moderate defect model with α=90° and β=45°, and large defect model with α=120° and β=45°.*

*Cup geometry*

The geometry of SeleXys PC® had been already reconstructed for a previous study, so the step file was imported in Abaqus/CAE (Figure 2.9).


*Figure 2.9 - CAD reconstruction of the SeleXys PC® acetabular cup. The outer diameter and the height of the cup are shown in the figure.*

### 2.2.2 Definition of the materials

The material behavior of the PU foam was considered linear elastic with an additional plasticity characterized with crushable foam definition and crushable foam hardening using the data from the Table 2.2.[87] Three different material densities, 15 pcf, 20 pcf, and 30 pcf, were considered in the FE simulations of the lever-out test while only the 15 pcf density was considered in the convergence analysis.

*Table 2.2 - Linear elastic and crushable foam plasticity parameters used for the material characterization*[87]

| | Poisson's ratio | Young's modulus (MPa) | Young's modulus (MPa) | Young's modulus (MPa) |
|---|---|---|---|---|
| **Linear elastic** | 0.001 | 128 | 230 | 391 |
| **PU foam density (pcf)** | | 15 | 20 | 30 |
| **Plasticity** | Uniaxial strain | Yield stress (MPa) | Yield stress (MPa) | Yield stress (MPa) |
| Crushable foam | 0 | 2.45 | 4.43 | 11.04 |
| | 0.01 | 3.90 | 6.80 | 13.29 |
| | 0.03 | 4.50 | 7.80 | 15.52 |
| | 0.05 | 4.51 | 8.20 | 16.51 |
| | 0.07 | 4.60 | 8.32 | 17.09 |
| | 0.10 | 4.51 | 8.52 | 17.64 |
| | 0.20 | 4.56 | 8.49 | 18.70 |
| | 0.40 | 5.00 | 9.20 | 22.00 |
| | 0.50 | 5.50 | 10.00 | 25.00 |
| | 0.60 | 6.00 | 11.30 | 30.00 |
| | 0.75 | 7.40 | 14.20 | 39.00 |
| | 1.00 | 12.00 | 21.00 | 63.00 |
| | 2.00 | 45.00 | 55.00 | 185.00 |

A linear elastic behavior with a Young's modulus of 110 GPa and a Poisson's ratio of 0.4 was assumed for the material characterization of the cup, made with Ti6Al7Nb alloy.[87]

### 2.2.3 Meshing and Convergence analysis

In the meshing process, linear hexahedral elements, C3D8R, were used for all the models. For the convergence study of the blocks, only the 15 pcf foam density definition was considered. All the blocks were partitioned along the symmetry planes and a radial displacement of 0.1 mm was applied to the cavity surface, defined imposing an angle of 27° between the superior plane and a line passing through the ideal center of rotation in the block. This was considered as the surface most subject (Region of interest, ROI) by a deformation during the insertion of the acetabular cup.[60]. A reference point (RP) was defined in the central point of the bottom

surface and it was coupled with a kinematic constraint to the bottom surface. An encastré boundary condition (x = y = z = rx = ry = rz = 0) was then applied to RP in order to fix the block (Figure 2.10).

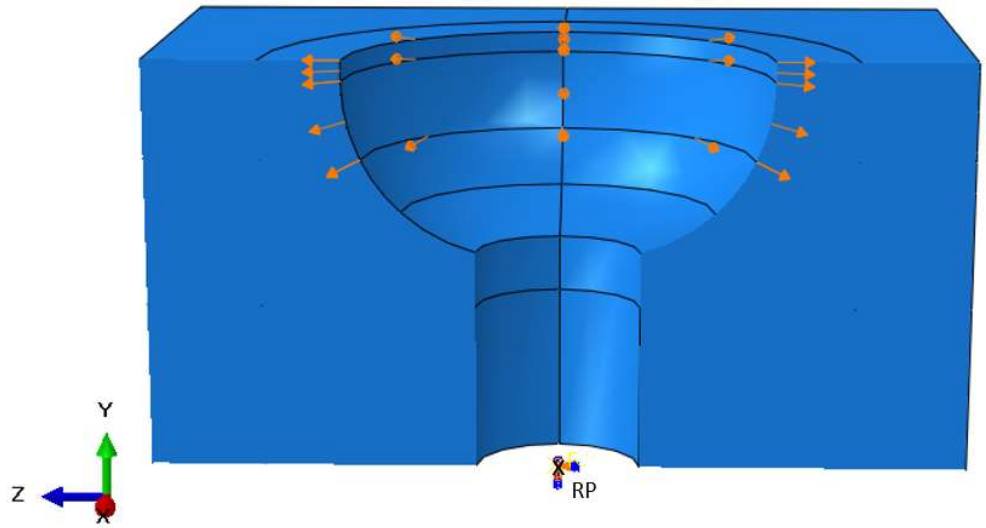


*Figure 2.10 - Block model with applied displacement and boundary condition: RP was fixed using an encastré while a radial displacement of 0.1 mm was applied to the surface of the cavity.*

Several analyses with increased mesh refinement were performed for the block models: eight for the intact cavity model, seven for the 90/45 defect model, and six for the 120/45 defect model. Firstly, a coarse mesh with a global edge length of 6 mm was generated. The local mesh refinements were then carried out in the area near the cavity. A cylindrical partition volume around the cavity with a radius of 10 mm greater than the rim was defined. The local refinement was led by assigning the local edge length to the edges around the cavity. The local edge lengths were 4 mm, 2 mm, 1.5 mm, 1.25 mm, 1 mm, 0.75 mm, and 0.5 mm. For the moderate and for the large defect models one or two of the last two refinements were not carried out, respectively. Two examples of the different meshes in the intact cavity model are depicted in Figure 2.11.

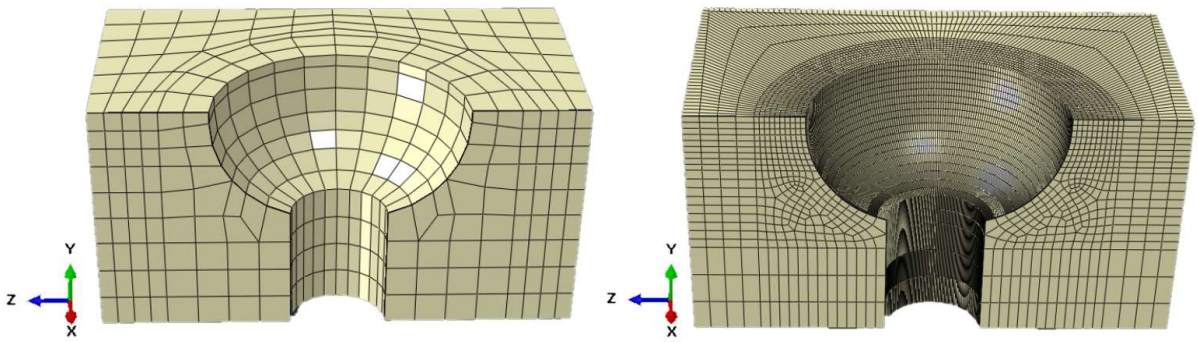


*Figure 2.11 - Intact PU foam block FE-model meshed with a global edge length of 6 mm (left) and with a local refinement of 0.75 mm (right).*

For the convergence analysis of the cup, a radial displacement of -0.1 mm, defined in a spherical reference system, was applied to the outer surface of the cup. A reference point was defined in the central point of the pole hole of the cup and it was coupled, as previously done for the block models, to the surface around the pole. An encastré boundary condition was applied to the reference point to fix the cup. The cup was partitioned in 8 identical segments along symmetry planes and the outer surface was also partitioned in order to define the surface interested by the displacement, using the same assumptions taken for the block. Eight analyses, with decreased global and local edge length, were performed for the cup. The global edge lengths were 6 mm, 4 mm, 2 mm, 1.5 mm, 1.25 mm, 1 mm, 0.75 mm, and 0.5 mm.
In Figure 2.12 two different meshes for the cup model are shown.

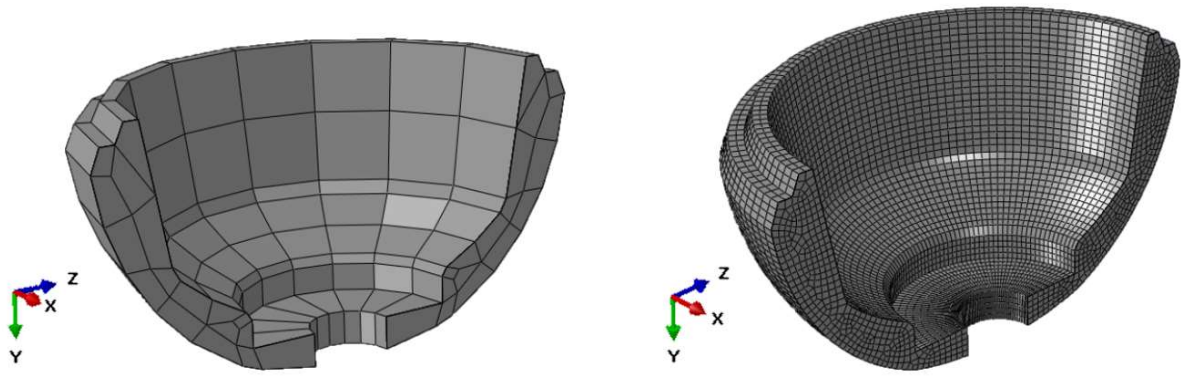


*Figure 2.12 - FE model of the cup meshed with a global edge length of 6 mm (left) and with a local refinement of 0.75 mm (right).*

The sum of the reaction forces along the radial direction, taken as the main parameter for the convergence studies, was calculated for all surfaces interesting for the evaluation of the displacement. For the main FE model, the blocks were meshed using a final element edge length of 1 mm while the cup with hexahedral elements of 1.25 mm.
The number of elements in each analysis is summarized in the table below (Table 2.3).

*Table 2.3 - Numbers of elements in the convergence analyses of the different block models and of the cup*

| | | Global edge length | | Local edge length in mesh refinements | | | | | |
|---|---|---|---|---|---|---|---|---|---|
| | | 6 | 4 | 2 | 1.5 | 1.25 | 1 | 0.75 | 0.5 |
| Numbers of elements | Intact block | 1860 | 6708 | 20364 | 30160 | 38952 | 49320 | 102984 | 192648 |
| | Defect 90_45 | 2365 | 7060 | 17389 | 22232 | 25100 | 52936 | 80630 | |
| | Defect 120_45 | 1760 | 6636 | 39600 | 60080 | 72300 | 102968 | | |
| | Cup | 288 | 432 | 2256 | 6528 | 9440 | 17760 | 46104 | 153504 |

For the main FE model, the blocks were meshed using a final element edge length of 1 mm while the cup with hexahedral elements of 1.25 mm.

### 2.2.4 Assembly, interactions, and boundary conditions

*Alignment of the model components*

The cup and the block were aligned inserting the cup in the block cavity without defining any contact, using the assembly constraints. The test protocol was reproduced with a quasi-static resolution in the FE simulations.

*Interaction definition*

The contact interaction between the outer surface of the cup and the cavity was modeled as a surface-to-surface contact, which describes contact between two deformable surfaces. The surface to surface contact requires a definition of a master and a slave surface as, by default, contact pairs in Abaqus/Standard use a pure master-slave contact algorithm. As the cup material had a higher relative stiffness than the PU foam of the block, the outer surface of the cup was selected as the master surface (Figure 2.13, red) and the block cavity as the slave surface (Figure 2.13, purple). For the interaction properties between the contacting surfaces, a penalty friction model was defined with Coulomb friction formulation for the tangential behavior and a hard contact pressure overclosure for the normal contact behavior. The friction coefficient was varied among 0.5, 0.6 and 0.7 for each cup-block combination. [77,88, 89,90]

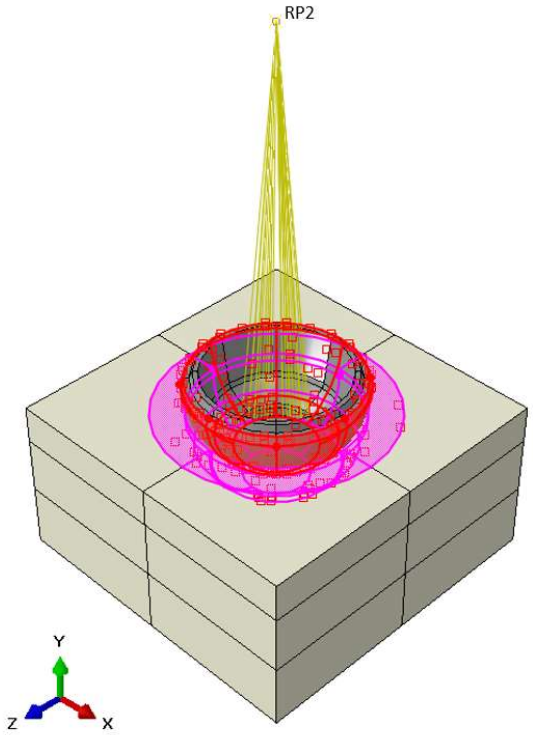


*Figure 2.13 – Contact interaction with the master surface highlighted in red and the slave surface highlighted in purple.*

Two reference points were defined and coupled, using a kinematic coupling, to the bottom surface of the block (RP1) and to the surface around the pole region of the cup (RP2)

respectively (Figure 2.14), to recreate the mounting of the block and the shaft used during the experimental tests.

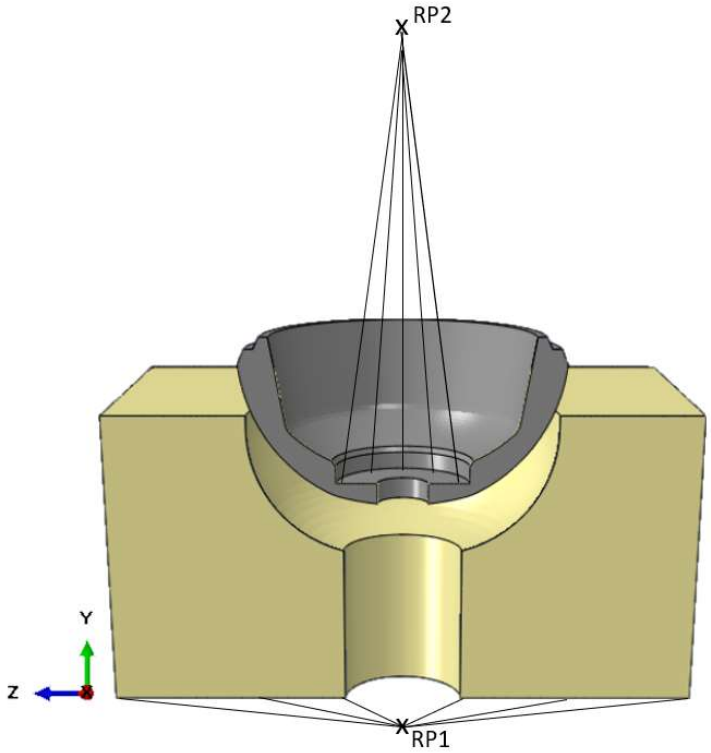


*Figure 2.14 – Schematic representation of the cup-block assembly with the reference points coupled to their respective surfaces in sectional view.*

*Boundary conditions*

An encastré boundary condition was defined in the "Initial" step for RP1 in order to fix the block, simulating the mounting process of the experimental insertion. Subsequently, the cup was inserted in the cavity, applying a displacement boundary condition to RP2 until the cup was fully seated, to perform the push-in test. The displacement during this process was allowed only in the y-direction. In order to simulate the worst scenario for the lever-out test, a displacement along the z-direction in the defect direction was then applied to the reference point until the contact between the cup and the cavity failed.

### 2.2.5 Step definition

The push-in test simulation was performed in four different steps (Figure 2.15). In the first insertion step "Initial contact", RP2 was displaced −4 mm along y-direction to reach the initial contact condition between the cup and the cavity. In the step "Push-in", the cup was moved until it is completely seated in the cavity imposing a further y-displacement by −4.5 mm. Finally, in the "Equilibrium" step, the boundary condition used to impose the y-displacement to the reference point was disabled to allow the system relaxation. In the last step of the simulation, "Lever-out", the cup was extracted.

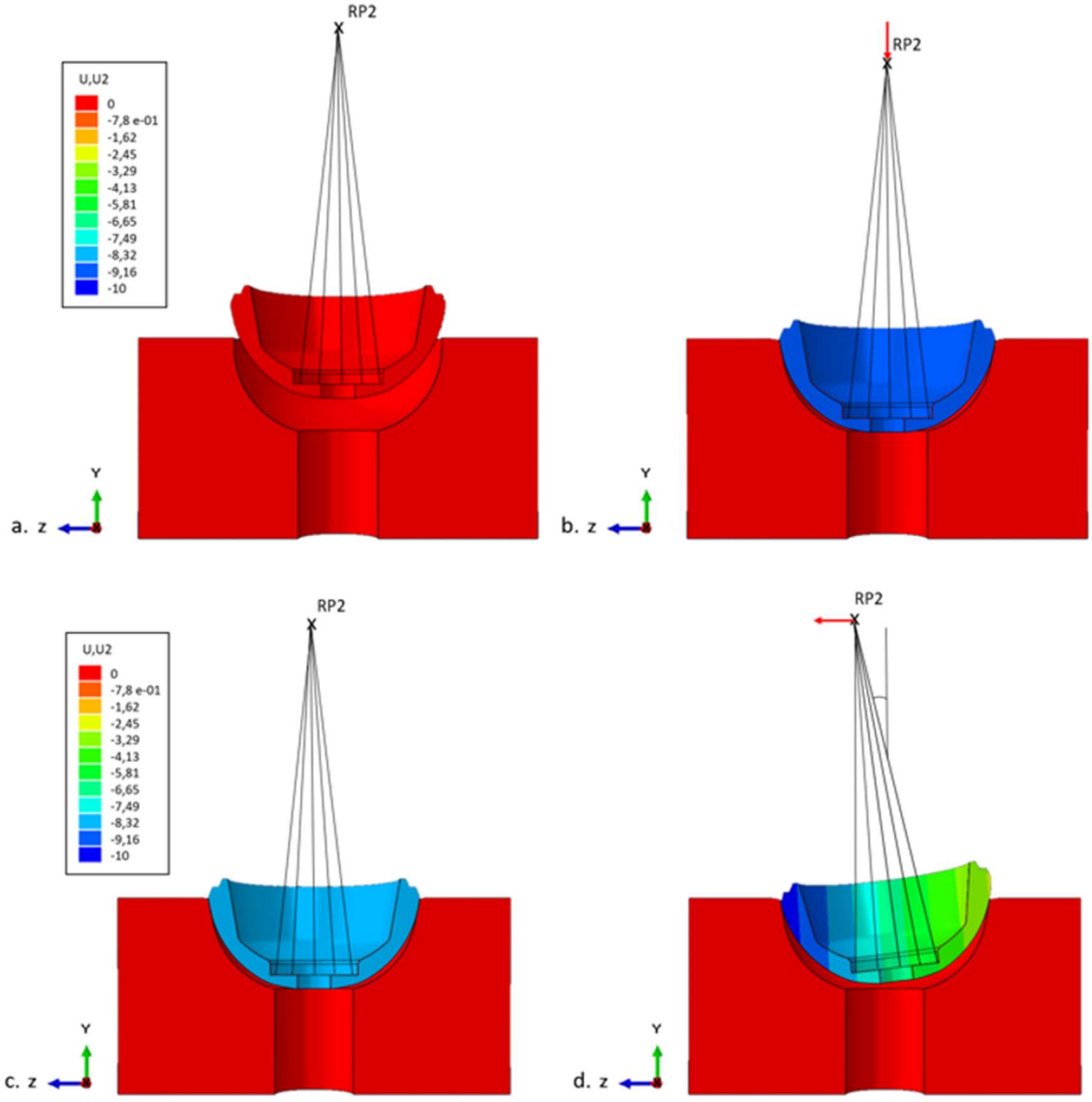


*Figure 2.15 – Schematic representation of the four simulation steps: a. Initial contact, b. Push-in, c. Equilibrium, d. Lever-out.*

The boundary conditions, applied to the RP2 in the different steps, are summed up in the table below.

*Table 2.4 – RP2 displacements in the different steps. The boundary condition "Push-in" reproduced the Push-in test; the boundary condition "Lever_out" replicates the Lever-out test*

| | Initial contact | Push-in | Equilibrium | Lever_out |
|---|---|---|---|---|
| Push-in | x = 0 mm<br>y = -4 mm<br>z = 0 mm | x = 0 mm<br>y = -8.5 mm<br>z = 0 mm | Inactive | Inactive |
| Lever_out | | | | z = 13 mm |

### 2.2.6 Analyzed parameters

The reaction forces and the displacements along y- and z-directions were determined during the simulations and were exported as a report file. Therefore, using Microsoft Excel v.1912 (Microsoft Corporation, Redmond, WA, USA), the mean and the standard deviation for the push-in and the lever-out forces were computed. The lever-out moments were calculated as previously described in the experimental test, without adding the moment due to the deadweight. The interface stiffnesses were also determined as the slope of the trend line in the first iterations of the force-displacement curve during the "lever-out" step. The total contact area was computed during the simulations and its influence on the other parameters was evaluated with a regression analysis.

Lastly, the contact pressures between the cup and the cavity were examined to determine the contact area location.

# 3. Results

The elaborated data of the experimental tests and the numerical simulations are illustrated in following subchapters.

## 3.1 Measurement of acetabular cups and artificial bone cavities

The actual diameters of the cups and of the reamed cavities are measured to evaluate whether the deviations from the nominal values could affect the results. The measured values are listed in Table 3.1. The deviations from the nominal reamed cavities are almost the same for all the block types, with larger deviations in the intact cavity blocks. Furthermore, a 1 mm difference between the diameters of the two different types of cups was determined.

*Table 3.1 - Evaluated diameters of the cups and of the reamed cavities in the Sawbones® blocks indicated as mean value ± standard deviation*

| | | Sawbones® blocks type | | |
|---|---|---|---|---|
| | Cup diameter | Intact cavity | Defect 90/45 | Defect 120/45 |
| Allofit® | 55.34 ±0.035 | 54.054 ±0.005 | 54.029 ±0.034 | 54.019 ±0.017 |
| TM™ | 56.4 ±0.042 | 54.084 ±0.062 | 54.030 ±0.034 | 54.022 ±0.015 |

## 3.2 Experimental tests

The results implemented by the data elaboration from the preliminary, the push-in, and the lever-out tests are delineated below.

### 3.2.1 Preliminary tests

The mean values of seating forces for the Allofit® and the TM cups in the different Sawbones® blocks are depicted in Figure 3.1. For all the PU foam blocks a larger force was needed by the TM cup in order to achieve the seating position computed as described in the material and method section. A decrease in the seating force with an increase of the defect size has been found for both the cups. The Allofit® shell shows a deviation from the seating force achieved in the intact cavity of 18% and 41% for the 90/45 defect and the 120/45 defect, respectively. The deviations in the TM cup are similar, with a decrease of 13% and 35% comparing the intact block with the 90/45 defect block and the 120/45 defect block, respectively.

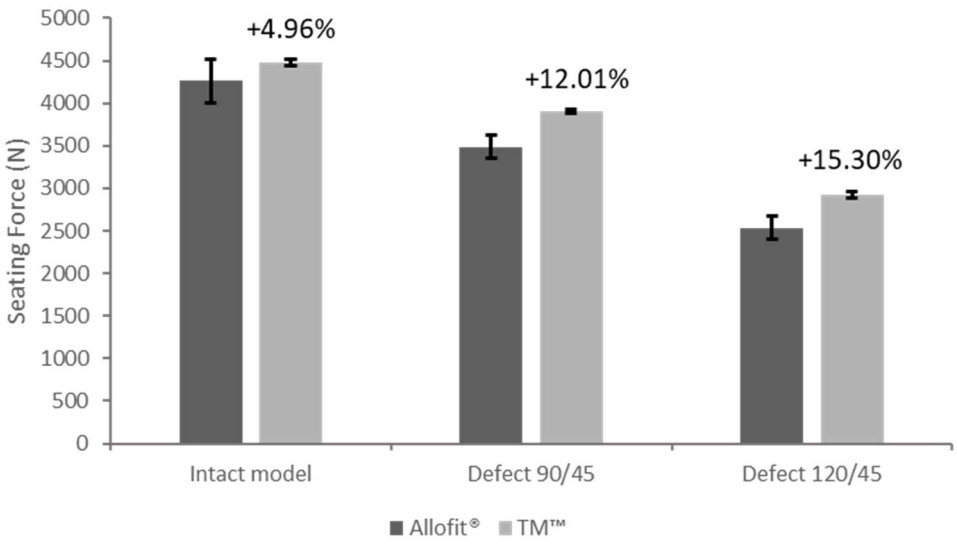


*Figure 3.1 - Seating forces of Allofit® Alloclassic® and TM™ cups in the three PU-foam blocks.*

### 3.2.2 Push-in tests

Two insertion curves that show the typical behavior of the two cups during the push-in test are depicted in Figure 3.2.

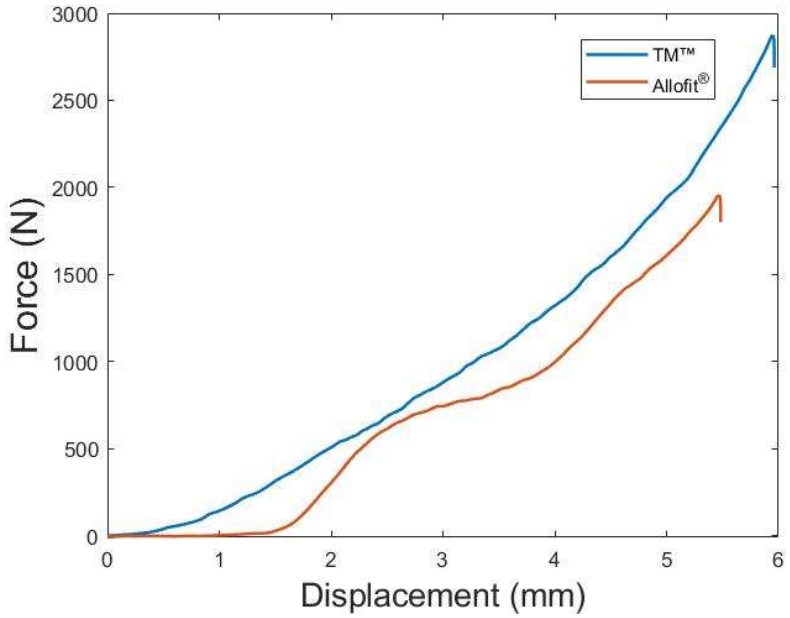


*Figure 3.2 - Force-displacement curves of the two Zimmer cups performing push-in tests in the block with the 120/45 defect.*

The dual geometry design of the Allofit® implant[79] (Figure 3.3, left) leads to an irregular trend due to the enlargement of the radius near the equator of the cup. The elliptical surface of the TM cup, on the contrary, exhibits a gradual transition in interference from the peripheral rim (2 mm) to the dome (0 mm) eliminating the discontinuities associated with the dual geometry design (Figure 3.3, right). The insertion curve of the TM cup shows indeed a smoother and almost exponential behavior.

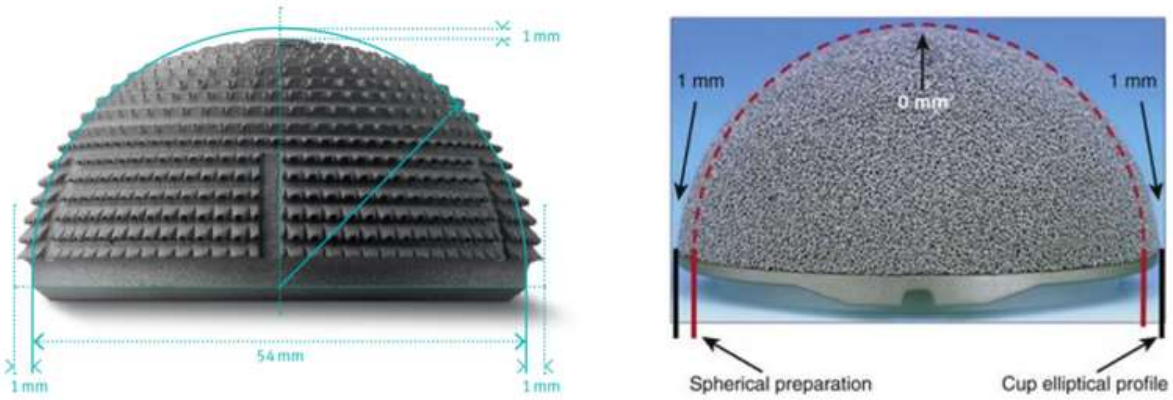


*Figure 3.3 - Outer surface design of the Allofit® cup (left)[91] and of the TM™ cup (right).[92]*

During the last push-in trial, performed with the Allofit® cup in the 90/45 defect block, an unexpected event caused the crush of the Sawbones® block. The lack of another block of the same type led to a smaller number of trials for that cup-block model.

The averaged insertion forces in the experimental push-in tests have a maximum value of 4514 N ± 451 N (intact cavity for the Allofit® cup) and a minimum value of 1778 N ± 189 N (defect 120/45 for the Allofit® cup) (Figure 3.4). By tendency, the push-in force decreased with increased defect sizes for both the cups. The deviation between the primary (Allofit®) and the revision (TM) cups is nearly zero in the intact cavity PU-foam block. A significant difference ($p<0.0008$) between the Allofit and the TM cup was found in presence of the large defect (120/45), where a deviation of the push-in force of 61 % was encountered.

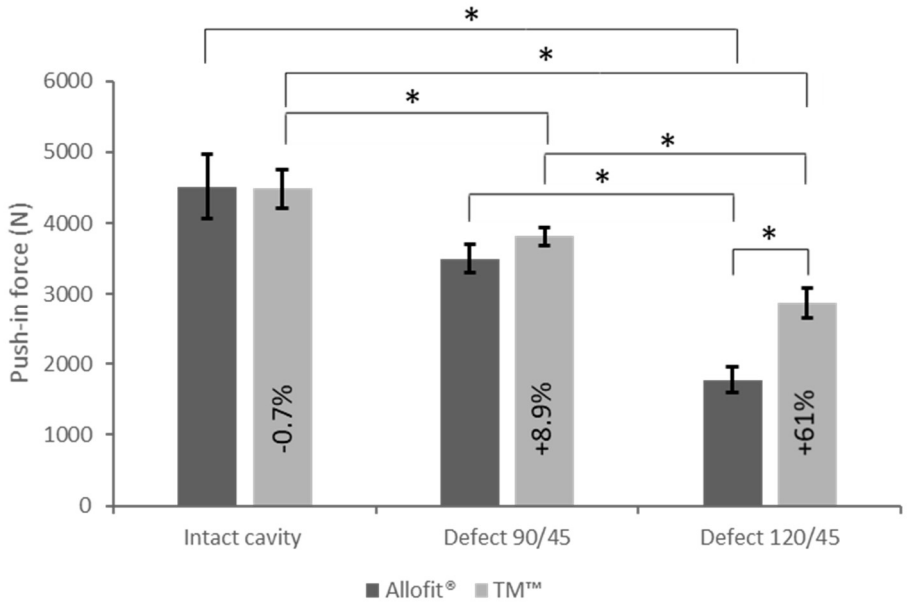


*Figure 3.4 - Push-in forces of the Allofit® and the TM™ cups in the different Sawbones blocks. The percentage deviations between the cups for the same block's type are indicated in the columns of the TM™ cup. To determine the significance levels, each type of Sawbones® block was compared to the others for the two different cups. Besides, the primary and the revision cup were compared for each type of block. A significance level of $p \leq 0.05$ was considered as statistically significant and was shown in the graph.*

### 3.2.3 Lever-out tests

*Lever-out moment*

The determined lever-out moments show a tendency similar to the push-in forces in the different defects. The range lies between 12.96 Nm ± 0.75 Nm (intact cavity for the TM™ cup) and 3.91 Nm ± 0.41 Nm (120/45 defect for the Allofit® cup) (Figure 3.5). The primary cup presents significantly reduced lever-out moments in the defects when compared to the intact cavity and the lever-out moment of the TM cup. The deviations between the intact cavity and the 90/45 defect are of 31.46% for the Allofit cup and 21.95% for the TM cup. Comparing the lever-out moment between the intact cavity and the 120/45 defect, the lever-out moment decreases by 66% ($p<0.016$) for the primary acetabular cup and by 39% ($p<0.0001$) for the revision cup.

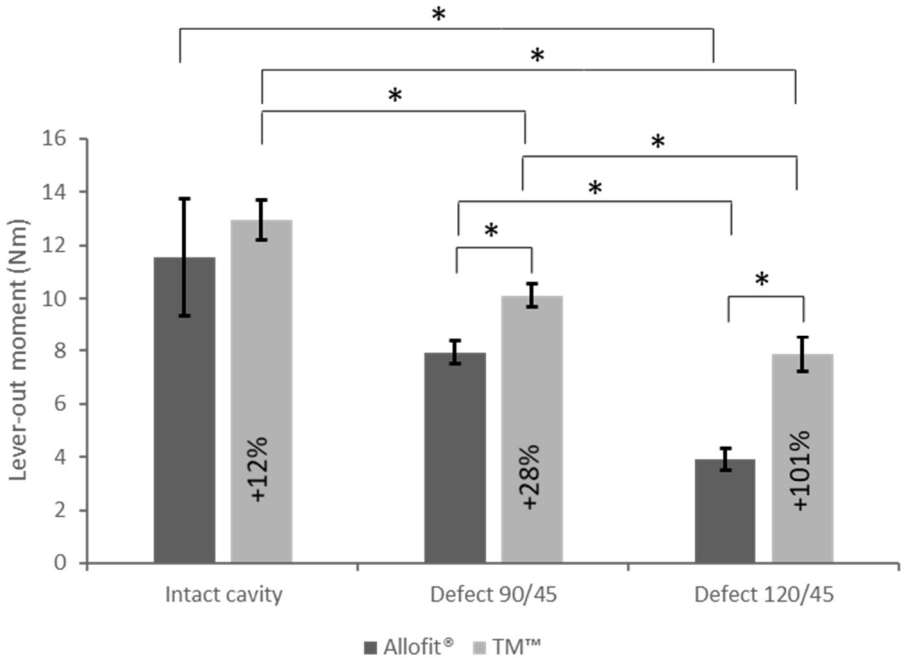


*Figure 3.5 – Lever-out moments of the Allofit® and the TM™ cups in the Sawbones blocks. The percentage deviations between the cups for the same block's type are indicated inside the columns of the TM™ cup. To determine the significance levels, each type of PU-foam block was compared to the others for the two different cups. Besides, the primary and the revision cup were compared for each type of block. A significance level of $p \leq 0.05$ was considered as statistically significant and was shown in the graph.*

*Interface stiffness*

Higher interface stiffnesses are found in all the Sawbones® blocks for the Allofit® cup. The two cups demonstrate a similar decrease in interface stiffness values as the defect extent increases (Figure 3.6). Deviations of 30.85% ($p<0.0019$) and 27.31% ($p<0.0009$) are reached comparing intact cavity and 90/45 defect for the Allofit® and the TM cup respectively, while reductions by 54.04% ($p<0.0034$) and 50.43% ($p<0.00002$) are found between the intact cavity and the 120/45 defect for the two different types of cup.

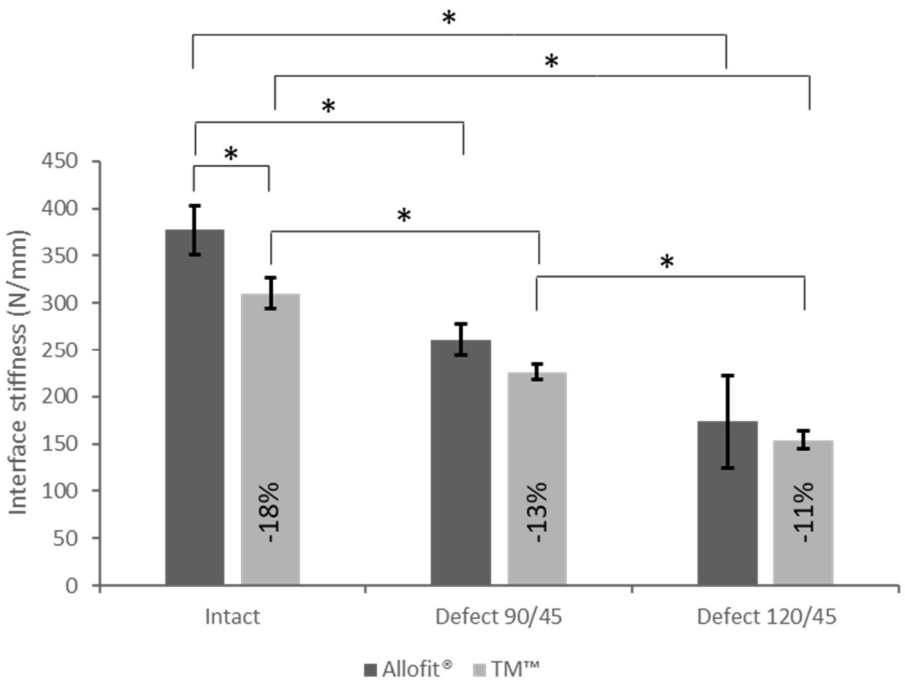


*Figure 3.6 – Interface stiffnesses of the Allofit® and the TM™ cups in the different PU-foam blocks. The percentage deviations between the cups for the same block's type are indicated in the columns of the TM™ cup. To determine the significance levels, each type of PU-foam block was compared to the others for the two different cups. Besides, the primary and the revision cup were compared for each type of block. A significance level of $p \leq 0.05$ was considered as statistically significant and was shown in the graph.*

*Lever-out work*

Small deviations have been found between the two cups in the intact and the smaller defect blocks, while in the 120/45 defect block the difference between the work values is significant. The TM cup achieves an almost constant value of the work in the three different Sawbones blocks, while the decrease of the studied parameter as the defect size increase is evident in the Allofit® cup (Figure 3.7).

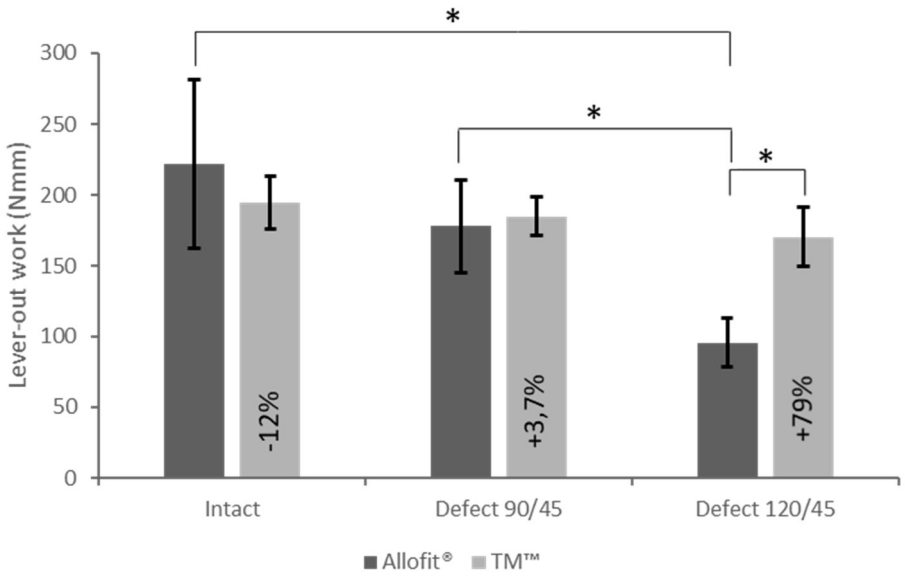


*Figure 3.7 – Lever-out works of the Allofit® and the TM™ cups in the different PU-foam blocks. The percentage deviations between the cups for the same block's type are indicated inside the columns of the TM™ cup. To determine the significance levels, each type of PU-foam block was compared to the others for the two different cups. Besides, the primary and the revision cup were compared for each type of block. A significance level of $p \leq 0.05$ was considered as statistically significant and was shown in the graph.*

*Regression analyses*

Two linear regression analyses were carried out to investigate a potential relationship between the lever-out moment and the interface stiffness with the corresponding push-in force (Figure 3.8). Both the parameters show a very strong correlation and high determination coefficient with the push-in force. A direct linear relationship between the push-in force and the other examined parameters is therefore established.

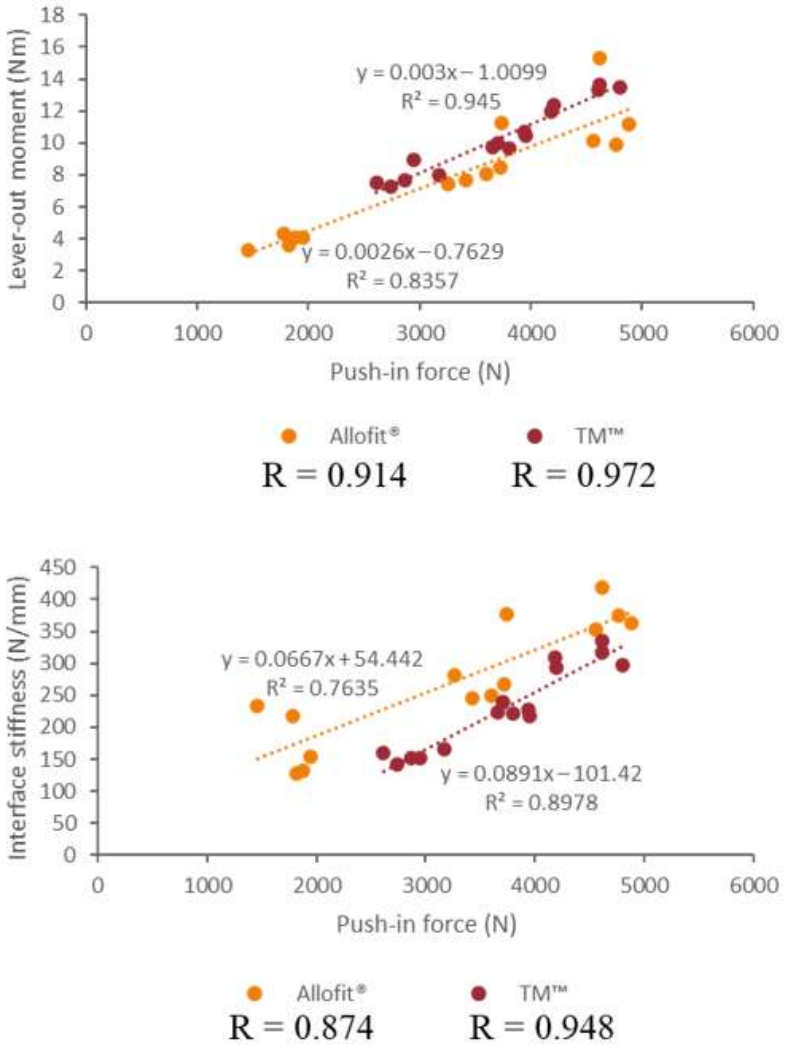


*Figure 3.8 - Regression analyses of the parameters. Lever-out moment vs push-in force (upper graph), interface stiffness vs push-in force (lower graph). The correlation coefficients are displayed under the legend.*

### 3.2.4 Visual analysis of the foam blocks

In order to investigate qualitatively the contact area extension in the different types of blocks, a visual examination after the cup extraction is conducted. Comparing the three pictures in Figure 3.9, it is noticeable that the contact area is homogenous in the intact cavity, while in the pictures b. and c., the contact area increases in the cavity region near the defects.

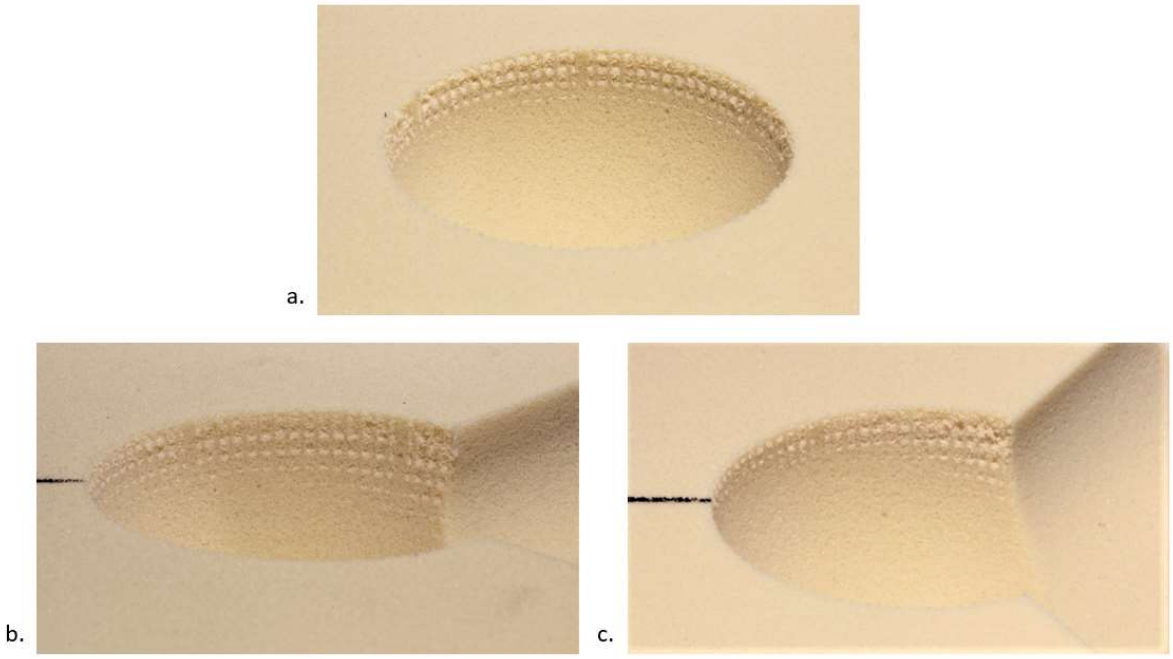


*Figure 3.9 – Sawbones blocks after the extraction of the Allofit® cup. a. Intact cavity, b. 90/45 defect and c. 120/45 defect.*

The abrasions caused by the TM cup in the foam blocks have a distribution similar to the Allofit® cup, but the region interested by the contact between the cup and the cavity seems to be smaller (Figure 3.10).

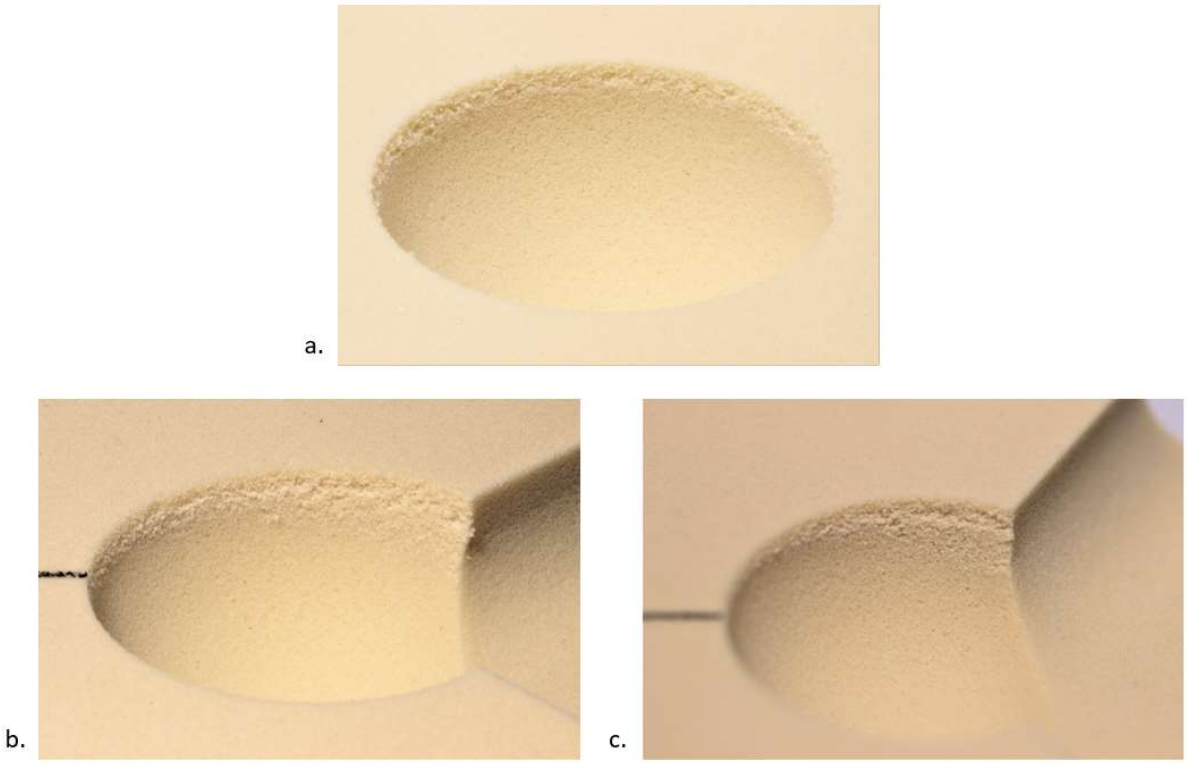


*Figure 3.10 - Sawbones blocks after the extraction of the TM™ cup. a. Intact cavity, b. 90/45 defect and c. 120/45 defect.*

## 3.3 Numerical simulations

The results obtained from the convergence analyses and from the cup-block FE models are illustrated in detailed below.

### 3.3.1 Mesh convergence analysis

The sum of the radial reaction forces and the computational time were evaluated according to the local edge lengths in mesh refinement for each PU-foam block model and for the cup (Figure 3.11).

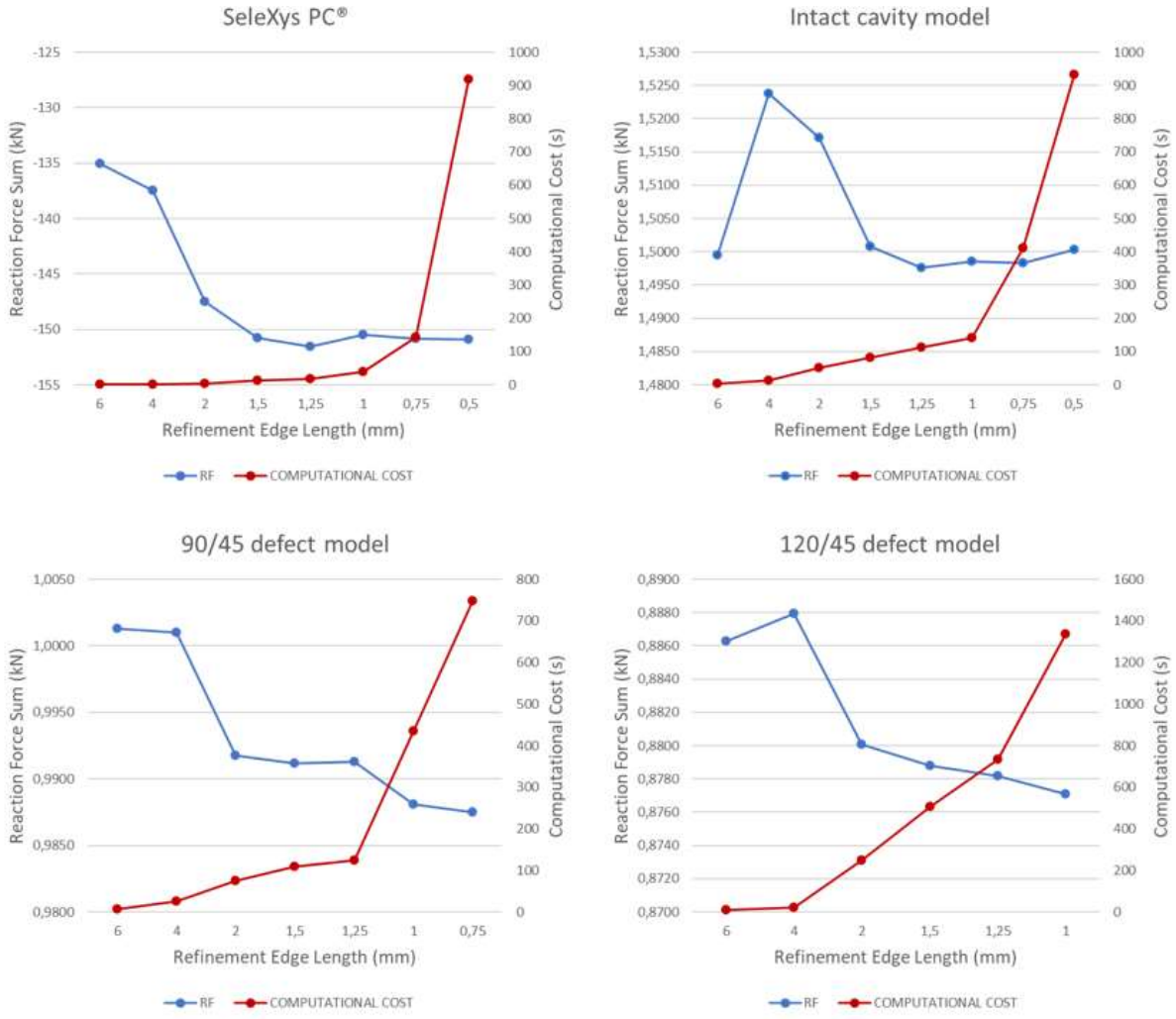


*Figure 3.11 – Radial reaction forces and computational costs for the cup and the PU foam block model related to the mesh refinements.*

Because of the difficulties in the refinement of the mesh for the larger defect block models (α=120°, β=45°), due to the sharp edges in the defect region, a local edge length of 1 mm was used to mesh all the PU foam block model in order to have congruent results between the simulations. The radial reaction force was affected by this choice by a percentage error lower than 0.2% for both the intact cavity model and the 90/45 defect model. Due to the surface to

surface contact interaction between the cup (master surface) and the cavity (slave surface), the cup was meshed, according to Abaqus/CAE User's Guide[93], with a coarser mesh, using a length of 1.25 mm for its elements to avoid excessive penetration of the master surface in the slave surface. The radial reaction force was affected by this choice by a percentage error lower than 0.5%.

### 3.3.2 Validation of FE model

The mean values of push-in forces and lever-out moments of the 15 pcf and the 30 pcf intact cavity FE models, obtained averaging their values for the different coefficients of friction, were compared to the experimental results in order to validate the FE models. The comparison between the push-in forces (Figure 3.12) shows greater values in the experimental results, with a larger deviation of 33% for the lower density model (15 pcf).

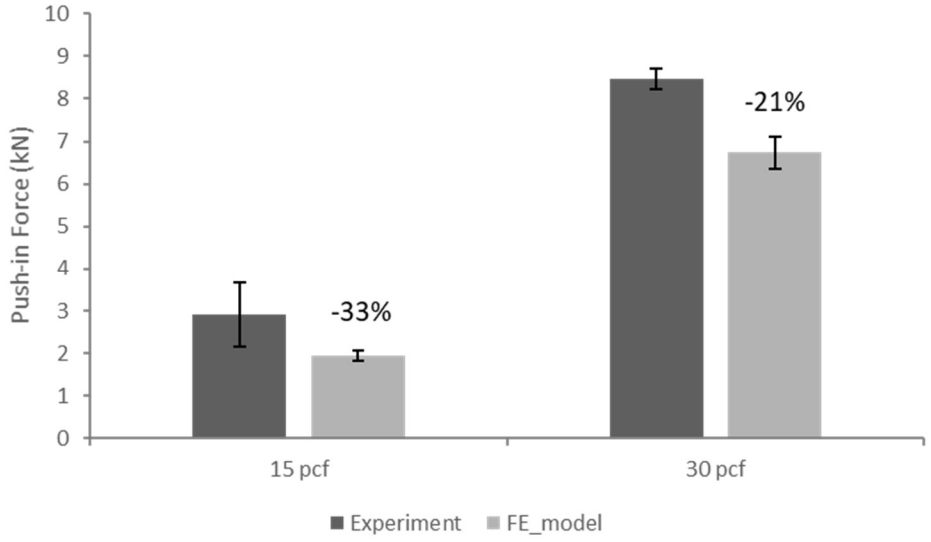


*Figure 3.12 - Comparison of push-in forces between experimental tests and FE models in different PU foam blocks.*

As for the push-in forces, the lever-out moments were greater in the experimental tests than in the FE models with a deviation of about 20% for both densities (Figure 3.13).

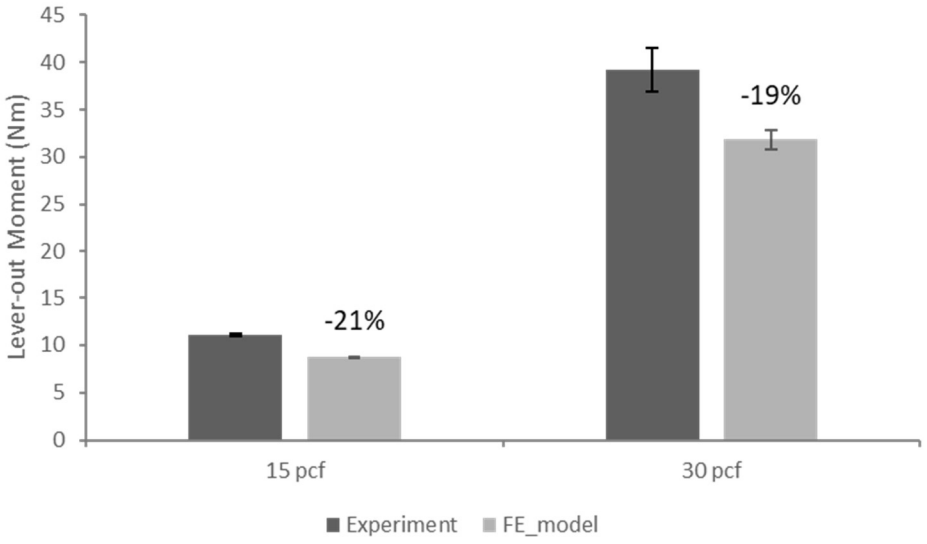


*Figure 3.13 - Comparison of lever-out moments between experimental tests and FE models.*

### 3.3.3 Comparison of push-in force between the three PU-foam block models

Six of the twenty-seven simulations were not completed successfully due to stability issues in contact interaction (Table 3.2).

*Table 3.2 - Summary of the unfinished simulations*

| | | Defect 90/45 | Defect 120/45 |
|---|---|---|---|
| | | Coefficient of friction | |
| Material density | 15 pcf | μ=0.5 | μ=0.5<br>μ=0.6<br>μ=0.7 |
| | 20 pcf | μ=0.5 | μ=0.5 |

The push-in force seems strongly related to the defect size and the material density (Figure 3.14). Between the 90/45 defect and the intact models a deviation of 22%, has been obtained in the 15 pcf and in the 20 pcf foam density, while in the 30 pcf PU foam the deviation is 16%. Between the 120/45 defect and the intact cavity models, a maximum deviation of 33% is reached for the 20 pcf density, whereas a 29% deviation is achieved in the 30 pcf block.

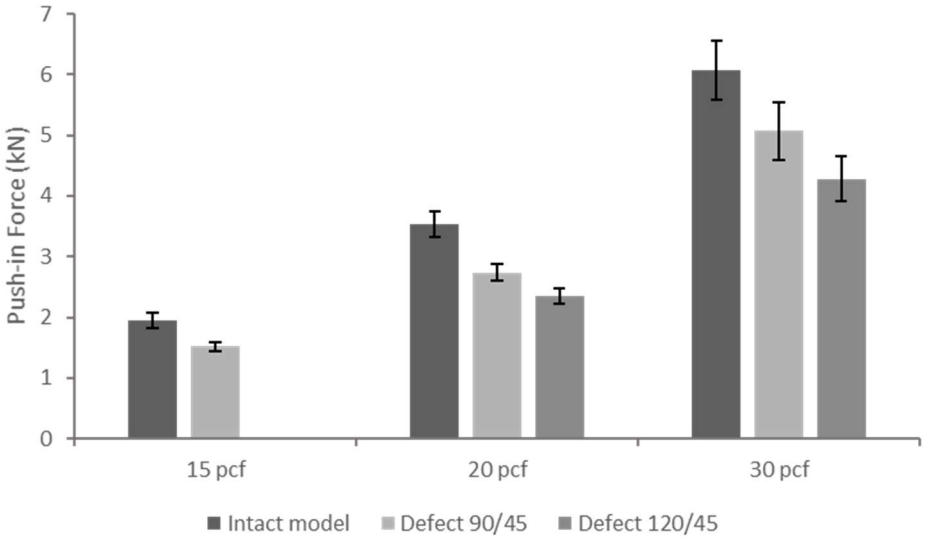


*Figure 3.14 – Comparison of the push-in force between the three PU-foam block models. The mean and the standard deviation are obtained averaging the values of the push-in forces for the different coefficients of friction (μ=0.5, 0.6, 0.7).*

### 3.3.4 Comparison of lever-out parameters

As for the push-in force, the values of the lever-out moment (Figure 3.15) and the interface stiffness (Figure 3.16) seem to be highly affected by the material density and by the size of the defects. Comparing the lever-out moments of the intact model and the ones of the 90/45 defect model, deviations of 46% for 15 pcf, 45% for 20 pcf, and 49% for 30 pcf are reached. The comparison of the lever-out moments between the intact cavity and the largest defect model leads to a deviation of 67% in the 30 pcf Sawbones® block and of 64% in the 20 pcf Sawbones® block.

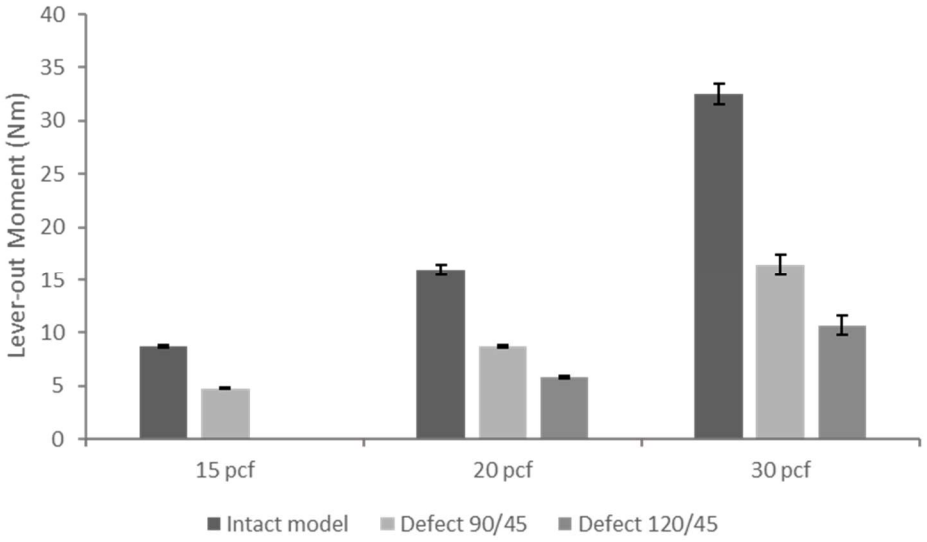


*Figure 3.15 - Comparison of the lever-out moment between the three PU-foam block models. The mean and the standard deviation are obtained averaging the values of the lever-out moment for the different coefficients of friction (μ=0.5, 0.6, 0.7).*

Similar deviation values are found for the interface stiffness with a maximum deviation of 49% obtained for the 30 pcf blocks between the intact model and the 90/45 defect model.

Comparing the intact model to the 120/45 defect model a maximum deviation of 65% is found in the 30 pcf block.

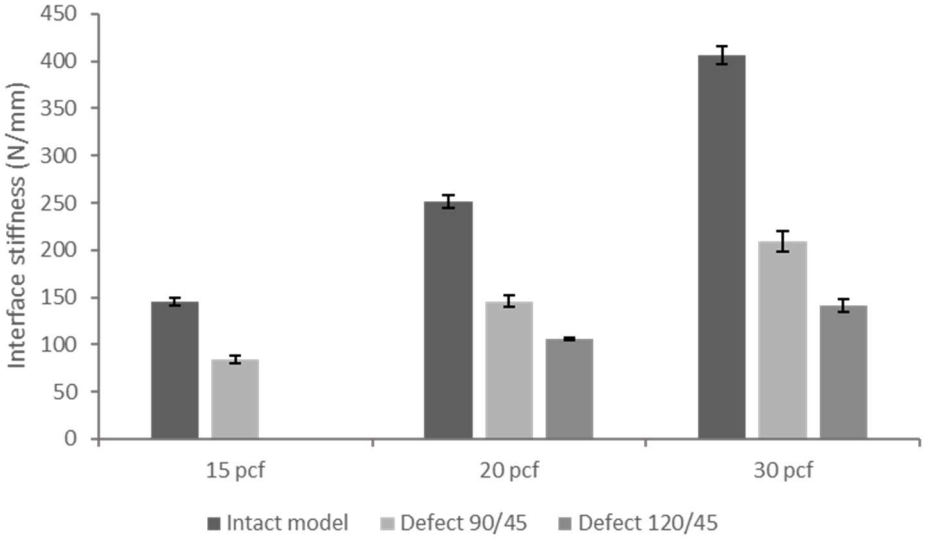


*Figure 3.16 – Comparison of the interface stiffness between the three PU-foam block models. The mean and the standard deviation are obtained averaging the values of the interface stiffness for the different coefficients of friction (μ=0.5, 0.6, 0.7).*

Furthermore, maintaining a constant defect size, an increase in the value of all the extracted parameters (i.e. push-in force, lever-out moment, and interface stiffness) with increasing foam densities can be observed. The deviations of the aforementioned parameters in the intact model between the 15 pcf and 30 pcf PU foam blocks lay in a range between 180% and 273%. Similarly, the deviation of the compressive modulus between the two PU foams is 205%. The accordance of compressive modulus and the deviations of the parameters between different densities can be also observed comparing 15 pcf and 20 pcf PU foam blocks. Indeed, as the compressive modulus of the foam raises from 128 MPa to 230 MPa with an increase of 79% of its value, the parameters have increments between 73% and 83%. Therefore, this analysis underlines a strong correlation between primary stability parameters and PU foam densities, showing a trend that can be useful to predict the behavior for different foam densities.

### 3.3.5 Contact area and contact pressure

A detailed analysis of the interface contact area between the cup and the PU foam block was conducted for the FE models to determine the influence of the size of the defects and the material density in the contact area and contact pressure distribution. All the parameters were extracted for the last increment of the "Equilibrium" step in which the cup was fully seated, and the balance between displacement-dependent forces and friction-dependent forces were found.

*Contact area*

Figure 3.17 depicts the total contact area (CAREA in Abaqus) for the three cup-block models and the different material densities. The parameter CAREA deviates between the intact cavity and the 90/45 defect cavity for 15 pcf foam and for 20 pcf foam by 31% and for 30 pcf foam by 27%. A decrease in the amount of contact area is evident even in the 120/45 defect. In this case the deviations from the intact cavity are 38% for the 20 pcf block and 49% for the 30 pcf block.

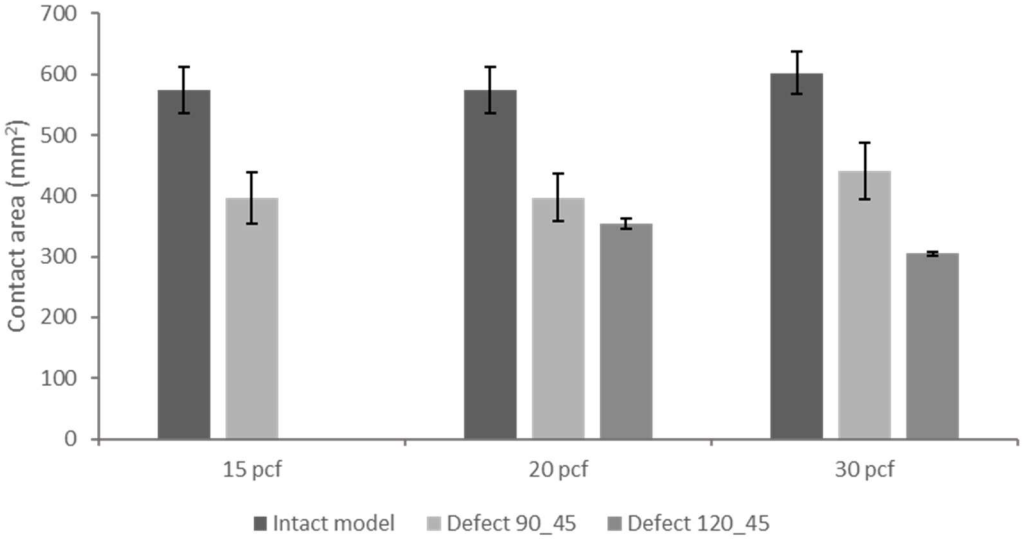


*Figure 3.17 – Comparison of the contact area between the three PU-foam block models. The mean and the standard deviation are obtained averaging the values of the contact area for the different coefficients of friction (μ=0.5, 0.6, 0.7).*

In the two figures below the local contact area (CSTATUS, Figure 3.18) and the local plasticity (PEEQ, Figure 3.19) of the PU-foam is visualized and the influence of the size of the defects can be analyzed. The contact between the cup and the block is localized on a narrow surface near the equator of the cavity. The same area is interested in a plasticity behavior with an increase in the plastic strain as the size of the defect increases ($PEEQ = 4.036 \times 10^{-1}$ in the intact cavity, $PEEQ = 9.478 \times 10^{-1}$ in the 120/45 defect).

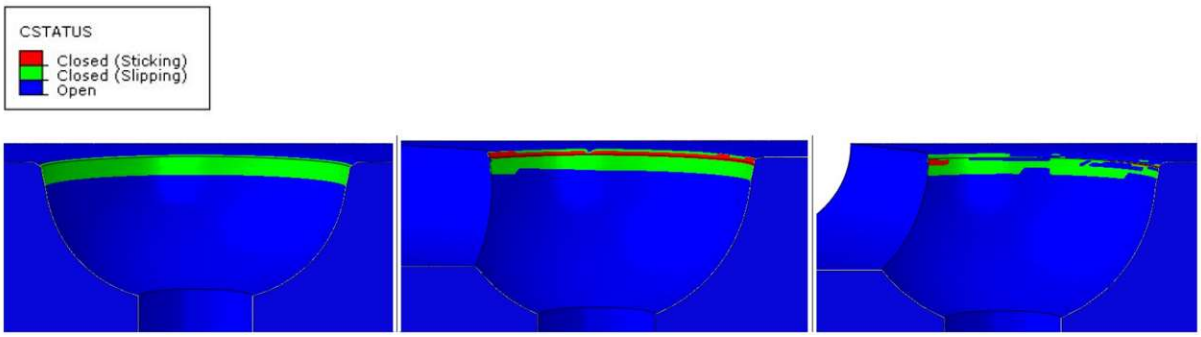


*Figure 3.18 - Contact status representing the contact area in the three defect models for the 30 pcf PU-foam block with a μ=0.6 coefficient of friction. From left to right: intact model, 90/45 defect model, and 120/45 defect model.*

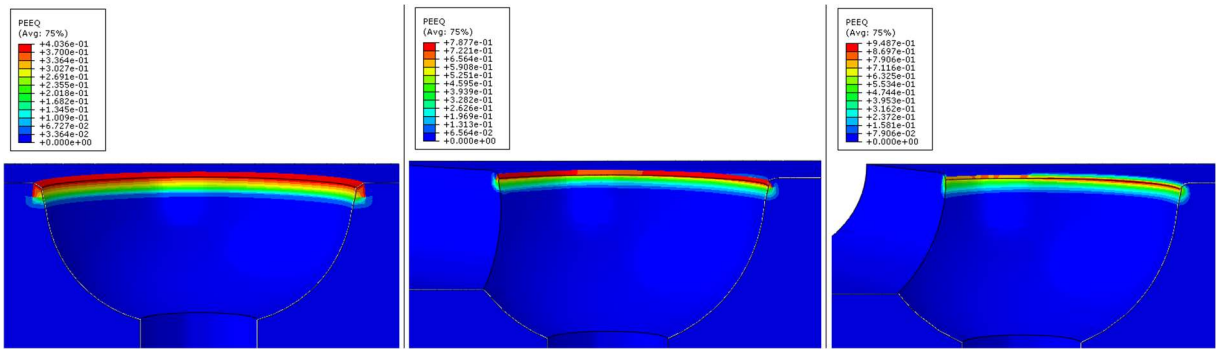


*Figure 3.19 - Equivalent plastic strain in the three defect models for the 30 pcf PU-foam block with a μ = 0.6 coefficient of friction. From left to right: intact model, 90/45 defect model, and 120/45 defect model.*

*Contact Pressure*

While the contact pressure is symmetrically distributed in the cavity for the intact model, with the appearance of the defects, the contact pressure is mostly concentrated near the defect area (Figure 3.20). Furthermore, the area subject to high contact pressure increases as the defect size increases.

The values assumed by the contact pressure are deeply influenced by the material density. In the intact model, for example, the CPRESS values range from 2.62 MPa to 13.59 MPa as the material density increases. The contact pressure (CPRESS in Abaqus) distribution is highly affected by the size of the defects.

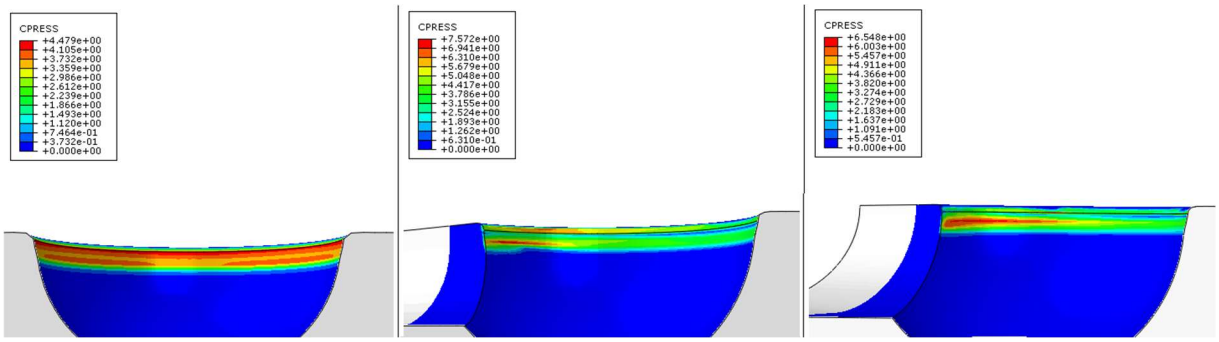


*Figure 3.20 – Comparison of contact pressure in different defect sizes for the 20 pcf PU-foam block with a μ = 0.6 coefficient of friction. From left to right: intact model, 90/45 defect model, and 120/45 defect model.*

The correlation coefficients between the previously determined parameters (push-in force, lever-out moment, and interface stiffness) and the extension of contact area computed in the FE simulation were calculated in order to evaluate if the contact area affects the primary stability of the cup (Table 3.3).

*Table 3.3 - Correlation coefficient between the contact area (x) and the primary stability parameters (y)*

| | 15 pcf | 20 pcf | 30 pcf |
|---|---|---|---|
| Push-in Force | 0.76 | 0.87 | 0.87 |
| Lever-out moment | 0.92 | 0.95 | 0.94 |
| Interface stiffness | 0.95 | 0.97 | 0.95 |

The values of the correlation coefficients reveal a very strong direct correlation between the contact area and the three parameters.

# 4. Discussion

The presence of acetabular segmental and superior defects is commonly encountered during revision THA. Different types of implants were developed in the last decades in order to manage the lack of bone stock and to restore the functionality of the hip joint.[18,45,51,56] The choice of implant can highly affect the long-term outcomes and it is often taken intraoperatively by the surgeon relying on his experience.

The aim of the experimental tests conducted in this Thesis work was to assess the primary stability of a primary and a revision cup design in the presence of different sizes of acetabular defects. The defects considered in this study simulate the loss of the superolateral bone stock of the acetabular cavity that can occur as a consequence of different pathologies (i.e. aseptic loosening of the implant, dysplasia, cysts formation). Lever-out tests were performed for the Allofit® and the Trabecular Metal™ cups using three different types of Sawbones blocks. The density of 0.32 g/cm$^3$, used in all the tests, replicates the density of a healthy bone, but cannot mimic completely the mechanical properties of human bone. The geometry of the acetabular cavity and of the defects was reconstructed using a CNC-machine. The diameters of the reamed cavities deviated by the nominal ones as depicted in Table 3.1. However, since the deviations were similar in all the blocks, the results were probably influenced in the same way in all the trials, and the comparisons between the performances of the cups in the different types of blocks can be therefore considered reliable.

Higher push-in forces and lever-out moments, as well as interface stiffnesses and lever-out work, were detected for both the cups in the intact cavity blocks, as expected. Indeed, the decrease in contact area especially in the superior portion highly affects the stability of a press-fit implant.[78,76] Furthermore, a higher primary stable fixation was achieved by the TM cup in both the defect types, comparing the push-in forces and lever-out moments of the two cups. Significant deviations were especially reached in the 120/45 defect, where the difference between the lever-out moments attained by the cups was 101% (Figure 3.5). This high deviation between the cups is probably due to the difference of press-fit interface as well as the different types of acetabular cup designs implants. The deviation of 1 mm between the diameters of two cups could strongly affect the results, as found in other studies where different interface fits were compared.[62,86,94] Moreover, good fixation in terms of primary stability for the TM cup in the presence of different types of defects was demonstrated in previous in vivo and in vitro studies.[62,95] The larger interface stiffness found for the Allofit cup seems to be in contrast with the other parameters that, as mentioned before, achieved higher values in the TM cup. The interface stiffness represents the resistance against the initial

movement of the implant due to the applied load. The main factor that affects this parameter for different cups inserted in the same substrate is, therefore, the macro and microstructure of the outer surface of the cup. The fine barb-shaped teeth that characterized the macrostructure of the Allofit shell abrade and deform the PU-foam during the insertion. The smoother highly porous microstructure of the TM cup provides a supportive environment to achieve bone ingrowth, whereas the primary stability is achieved thanks to a high coefficient of friction between the implant and the cavity due to the press-fit. Moreover, due to the push-in method used according to Small et al., we do not know the effective press-fit achieved after the cup insertion. The differences in the abrasion traces left in the PU-foam blocks after the extraction of the two cups are shown in the pictures in the Appendix A and highlight the different extension of the contact area for the two cups.

The values of the push-in force may have been deeply affected by the method used to determine the seating position of the cup. This method, based on Small et al., divided the force-displacement curves, acquired during the insertion of the cup, in three main regions: a linear translation phase, a toe region, and a final linear region.[64] The seating force is therefore determined by shifting the final linear region that is assumed to be governed only by the compressive modulus of the block as explained in Section 2.1.3. Looking at the implantation curves obtained during the insertion of the two Zimmer cups (Figure 3.2), the three regions cannot be easily identified, especially in the Allofit® curve that exhibits an irregular trend. Thus, the final positions computed with this method differ from each other, especially between the different block types and probably affect the cups' performances. Furthermore, the 'bounce-back' that characterizes the cup implantation was not taken into account during the estimation of the seating positions. The deviations of the final position from the optimum seating position could have slightly influenced even the lever-out moment, changing the center of rotation of the cup during the tests. However, the difference between the actual and the measured lever-out arm is probably less than 0.5 mm and can, therefore, be neglected. Despite these limitations, the values of the aforementioned parameters, recorded during the experimental tests, are in good agreement with the results available in the literature.[78,96] For both cups, a strong linear relationship between the push-in force and the lever-out moment, as well as the interface stiffness, was discovered (Figure 3.8). This outcomes are consistent with the deductions of previous findings.[78,96]

By implementing the statistical analysis on the data, a high standard deviation was observed for both the lever-out moment and work, in the second trial for the intact cavity block of the Allofit® cup. Examining the box plot diagram in the SPSS outcomes, these values were

labeled as outliers. However, since an exclusion protocol for possible outliers was not contemplated in the analysis design, the whole data from that trial were taken into account in the statistical analysis and may have changed the significance levels between the data. The cause of these outliers can be searched in a deviation of the foam density. Measuring the artificial bone blocks' weights, the largest standard deviation within the blocks of the same type was found in the intact cavity blocks used for the Allofit® cup. In particular, the block that had a larger deviation from the mean value was the one that had caused the outlier value for the lever-out moment and for the lever-out work mentioned before.

There are many differences between the experimental conditions in which the tests were performed and the clinical environment. Two of the limitations are the idealization of acetabular cavities and bone conditions. The use of CNC milled cavities simplifies the acetabulum geometry and does not consider important anatomical features. This idealization of the acetabular cavities leads to an overestimation of the initial stability of the press-fit cups.[76] Furthermore, the adoption of the artificial bone is mandatory in order to promote the repeatability of the tests but neglects the viscoelastic characteristics, as well as the heterogeneous and anisotropic behavior of the trabecular bone tissue. The insertion of the cups, under displacement-controlled conditions, is another simplification needed to have reproducible experimental conditions whereas, interoperative hammer impaction is a highly dynamic process that can cause a stiffening in the bone due to a viscoelastic response.[77,97] However, the purpose of this Thesis was to compare the behavior of the different types of implant in the presence of different sizes of acetabular defects rather than their in vivo behavior and performance. Performing all the tests using the same protocol and the same boundary conditions the results of the different cup-block models are comparable.

A FE model of a cup block assembly using a different cup (SeleXys PC), during the lever-out process, was created and validated to investigate the influence on the initial stability of parameters that are difficult to analyze experimentally, such as the contact area and contact pressure. A big advantage of numerical simulations compared to experimental tests is the amount and the variety of parameters analyzable at once. The results of the numerical simulation can be useful especially when limited experimental tests can be achieved and can lead to the optimization of the experimental setup. However, computational modeling is subject to many limitations related to the simplifications of the reality that must be taken to create the FE model.

In the present model, one of the main limitations is related to the geometry of the cup's outer surface and the block's cavity. The high porosity of the outer surface of the SeleXys® cup was

only partially included in the coefficient of friction in the contact interaction between the cup and the cavity of the PU-foam blocks. Furthermore, the reamed cavities in the real blocks can have dimension deviations due to the reaming process and to the foam porosity that was not considered in the model. Knowing the limitations of the FE model is essential, to analyze and to interpret the results of the numerical simulation.

In the validation of the intact block model, deviations between 21% and 33% were found for the push-in force, while deviations between 19% and 21% were achieved for the lever-out moment for the 15 pcf ad the 30 pcf, respectively. Schulze et al. and Souffrant et al. obtained similar deviations in their studies, and the results were therefore considered consistent and the FE model validated.[87,88] The deviations can be due by the geometries simplifications displayed above, but another simplification that can have affected the results is related to the coefficient of friction. The penalty formulation of the contact interaction considers a static coefficient of friction that remains constant during the simulation. During the experimental tests, the coefficient of friction may not remain constant as the PU-foam cells collapse during the insertion and the lever-out processes. A dynamic coefficient of friction could be therefore considered, in order to take into account plasticity phenomena that can occur during the insertion and the lever-out of the cup.

Moreover, a finer mesh density could diminish the deviations between the model and the experimental results. For the intact FE model, a refinement of the mesh was not carried out to have consistent results with the models of the defect blocks. The sharp geometries of the area around the defect led to many difficulties during the mesh refinement process for both defect sizes. Although a partitioning procedure has been accomplished on the part, it was not possible to achieve a local refinement lower than 1 mm of local edge length for the 120/45 defect block, using the hexahedral element. In order to achieve a finer mesh density, tetrahedral elements might be used. Tetrahedral elements are the most flexible type of element and are usually used with complicated geometries. On the other hand, this type of elements seems to achieve a worse result compared with the hexahedral elements, especially in frictional contact models or in dynamic conditions.[75,98,99] A different geometry reconstruction of the area around the defect in the block or a different meshing technique (i.e. bottom-up or sweep loft) could also lead to better results in the mesh refinement process and might reduce the contact instabilities in the simulations that caused the abortion of some of the simulations.

A validation for the two FE defect model was not possible due to the lack of experimental data. The deviations from the real cup-block model for these two models could be worse than the ones of the intact model because of the mesh issues pointed out above. However, the use

of a validated FE model as a baseline in order to conduct analyses changing only a few parameters (e.g. the geometry and the material densities) was found in other studies.[86,100] Furthermore, these numerical models aimed to compare the primary stability in the presence of an increase of the size of the defect, identifying potential trends, so the congruency between the three FE models allows the comparison between the simulations results.

Comparing the push-in force, the lever-out moment, and the interface stiffness in the three models, a decrease in all the parameters is observed as the size of the defects increases. The parameters are also affected by the material density, with an increase in their values as the PU-foam becomes stiffer. The lever-out moment obtained in the intact model is in good agreement with the results obtained in a previous study, considering the different density of the material and the different friction coefficient used in their model.[96]

In the evaluation of the contact area and in the analysis of the contact area distribution the results seem to confirm the observations of other studies and of the experimental results of this Thesis, finding only a narrow equatorial area interested in the contact between the cup and the reamed cavity. [86,96,101] Moreover, the contact area seems to be highly affected by the presence of the defect (Figure 3.18), and its homogeneous distribution around the rim decreases as the defect size increases. The influence of the amount of contact area between the cup and its support on the primary stability of the implant finds a confirm in the correlation coefficient found in this Thesis (Table 3.3).

# 5. Conclusion

The experimental tests and the numerical simulations performed in this work underline how the presence and the extension of acetabular defects can affect the primary stability of an acetabular implant. The two types of investigations agree with each other regarding the contact area distribution and the trend of all the parameters with an increase in the sizes of defects. Furthermore, the comparison between the primary and the revision implant pointed out how the choice of the implant can deeply affect the surgery outcomes. This is a critical aspect, especially in the presence of a large defect in which the peripheral contact between the cup and the cavity is compromised by the missing superior rim support.

Future studies could deepen the comparisons between the different types of implants, using different testing methods and developing FE models for the Zimmer cups.

# Bibliography


1. Blaisdell, F. & Anthony, C. P. Structure and Function of the Body. *Am. J. Nurs.* **69**, 1075 (1969).
2. Chaitow, L., DeLany, J., Chaitow, L. & DeLany, J. Chapter 12 – The hip. *Clin. Appl. Neuromuscul. Tech. Vol. 2* 391–445 (2011) doi:10.1016/B978-0-443-06815-7.00012-7.
3. Hip Displasia pada Anak. http://www.syauqiya.com/2016/08/hip-displasia-pada-anak.html.
4. Fagerson, T. L., Babatunde, O. M. & Safran, M. R. Hip Pathologies. *Pathol. Interv. Musculoskelet. Rehabil.* 651–691 (2016) doi:10.1016/b978-0-323-31072-7.00018-x.
5. Laurence, W. Osteoarthritis of the Hip. *Br. Med. J.* **1**, 1893 (2011).
6. Lespasio, M. J. *et al.* Hip Osteoarthritis: A Primer. *Perm. J.* **22**, 89–94 (2018).
7. Bicanic, G., Barbaric, K., Bohacek, I., Aljinovic, A. & Delimar, D. Current concept in dysplastic hip arthroplasty: Techniques for acetabular and femoral reconstruction. *World J. Orthop.* **5**, 412–424 (2014).
8. Garabekyan, T., Chadayammuri, V., Pascual-Garrido, C. & Mei-Dan, O. Arthroscopic Bone Grafting of Deep Acetabular Cysts Using a Curved Delivery Device. *Arthrosc. Tech.* **5**, e113–e119 (2016).
9. Cornell, T. Ankylosing spondylitis: an overview. *Prof. Nurse* **19**, 431–432 (2004).
10. Jergersen, S. Total hip arthroplasty. *West J Med* 243–249 (1995) doi:10.1017/CBO9781316145227.019.
11. Smith & Nephew. Total Hip Replacement. https://bonesmart.org/hip/total-hip-replacement-surgery/.
12. Charnley. Arthroplasty of the hip. *Lancet* 1129–1132 (1961).
13. Toossi, N. *et al.* Acetabular components in total hip arthroplasty: Is there evidence that cementless fixation is better? *J. Bone Jt. Surg. - Ser. A* **95**, 168–174 (2013).
14. Kraay, M. J., Rowbottom, J. S. & Razek, M. G. The Acetabular Component in Primary Total Hip Arthroplasty. *Semin. Arthroplasty* **23**, 163–166 (2012).
15. Lee, J.-M. The Current Concepts of Total Hip Arthroplasty. *Hip Pelvis* **28**, 191 (2016).
16. Saleh, K. J., Bear, B., Bostrom, M., Wright, T. & Sculco, T. P. Initial Stability of Press-Fit Acetabular Components: An In Vitro Biomechanical Study. 519–522 (2008).
17. Karuppal, R. Biological fixation of total hip arthroplasty: Facts and factors. *J. Orthop.* **13**, 190–192 (2016).
18. Shon, W. Y., Santhanam, S. S. & Choi, J. W. Acetabular reconstruction in total hip arthroplasty. *Hip Pelvis* 1–14 (2016) doi:10.1097/00001433-199702000-00001.

19. Wasielewski, R. C., Cooperstein, L. A., Kruger, M. P. & Rubash, H. E. Acetabular anatomy and the transacetabular fixation of screws in total hip arthroplasty. *J. Bone Jt. Surg. - Ser. A* **73**, 1272 (1990).
20. Yin, X. *et al.* Screw-hole clusters in acetabular cups: A morphological study of optimal positioning of screw-holes. *HIP Int.* **27**, 382–388 (2017).
21. Pilliar, R. M., Lee, J. M. & Maniatopoulos, C. Observations on the effect of movement on bone ingrowth into porous-surfaced implants. *Clinical Orthopaedics and Related Research* vol. NO. 208 108–113 (1986).
22. van der Merve, J. M., Garbuz, D. S., Duncan, C. P. & Masri, B. A. Periprosthetic Fractures of the Femur Associated with Hip Arthroplasty. (2016).
23. Chitre, A., Wynn Jones, H., Shah, N. & Clayson, A. Complications of total hip arthroplasty: Periprosthetic fractures of the acetabulum. *Curr. Rev. Musculoskelet. Med.* **6**, 357–363 (2013).
24. Hanssen, A. D. Intraoperative fractures during primary total hip arthroplasty. *Orthopedics* **29**, 785–786 (2006).
25. Kwon, M. S. *et al.* Does surgical approach affect total hip arthroplasty dislocation rates? *Clin. Orthop. Relat. Res.* 34–38 (2006) doi:10.1097/01.blo.0000218746.84494.df.
26. Rapjura; Board. Complication following total hip athroplasty. *Intech Open* 381–419 (2013).
27. Baharuddin, M. Y. & Kadir, M. R. A. Finite Element Study on the Stability of Cementless Acetabular Cup. *IFMBE Proc.* **31**, 601–604 (2010).
28. Varacallo M, J. N. Total Hip Arthroplasty (THA) Techniques. in *StatPearls* (2019).
29. Nutt, J. L., Papanikolaou, K. & Kellett, C. F. Complications of total hip arthroplasty. *Orthop. Trauma* **27**, 272–276 (2013).
30. Kokubo, Y. *et al.* Long-term clinical outcome of acetabular cup revision surgery: comparison of cemented cups, cementless cups, and cemented cups with reinforcement devices. *Eur. J. Orthop. Surg. Traumatol.* **26**, 407–413 (2016).
31. D'Antonio, J. A. *et al.* Classification and management of acetabular abnormalities in total hip arthroplasty. *Clin. Orthop. Relat. Res.* 126–137 (1989) doi:10.1097/00003086-198906000-00019.
32. Macheras, Baltas & Kostakos. Management of large acetabulum defects. *Acta Orthop Traumatol Hell* (2003).
33. Paprosky, W. G., Perona, P. G. & Lawrence, J. M. Acetabular defect classification and surgical reconstruction in revision arthroplasty. A 6-year follow-up evaluation. *J. Arthroplasty* **9**, 33–44 (1994).

34. Telleria, J. J. M. & Gee, A. O. Classifications in brief: Paprosky classification of acetabular bone loss. *Clin. Orthop. Relat. Res.* **471**, 3725–3730 (2013).
35. Saleh, K. J. *et al.* Development, test reliability and validation of a classification for revision hip arthroplasty. *J. Orthop. Res.* **19**, 50–56 (2001).
36. Parry, M. C. *et al.* A comparison of the validity and reliability of established bone stock loss classification systems and the proposal of a novel classification system. *HIP Int.* **20**, 50–55 (2010).
37. Boscainos, P. J., Kellett, C. F., Maury, A. C., Backstein, D. & Gross, A. E. Management of periacetabular bone loss in revision hip arthroplasty. *Clin. Orthop. Relat. Res.* 159–165 (2007) doi:10.1097/BLO.0b013e3181560c6c.
38. Makinen, T. J., Kuzyk, P., Safir, O. A., Backstein, D. & Gross, A. E. Current concepts review: Role of cages in revision arthroplasty of the acetabulum. *J. Bone Jt. Surg. - Am. Vol.* **98**, 233–242 (2016).
39. Campbell, D. G., Garbuz, D. S., Masri, B. A. & Duncan, C. P. Reliability of acetabular bone defect classification systems in revision total hip arthroplasty. *J. Arthroplasty* **16**, 83–86 (2001).
40. Yu, R. *et al.* Validity and reliability of the paprosky acetabular defect classification hip. *Clin. Orthop. Relat. Res.* **471**, 2259–2265 (2013).
41. Safir, O. *et al.* Limitations of conventional radiographs in the assessment of acetabular defects following total hip arthroplasty. *Can. J. Surg.* **55**, 401–407 (2012).
42. Garcia-Cimbrelo, E., Tapia, M. & Martin-Hervas, C. Multislice computed tomography for evaluating acetabular defects in revision THA. *Clin. Orthop. Relat. Res.* 138–143 (2007) doi:10.1097/BLO.0b013e3181566320.
43. Hettich, G. *et al.* Method for quantitative assessment of acetabular bone defects. *J. Orthop. Res.* **37**, 181–189 (2019).
44. Della Valle, C. J., Berger, R. A., Rosenberg, A. G. & Galante, J. O. Cementless Acetabular Reconstruction in Revision Total Hip Arthroplasty. *Clin Orthop* 96–100 (2004).
45. Reid, C., Grobler, G., Dower, B., Nortje, M. & Walters, J. Revision total hip arthroplasty: addressing acetabular bone loss. *SA Orthop. J.* **11**, 34–46 (2012).
46. Blumenfeld, T. J. Implant choices, technique, and results in revision acetabular surgery: A review. *HIP Int.* **22**, 235–247 (2012).
47. Dankl, L. *et al.* Measuring bone defects for acetabular revision surgery for choosing an appropriate reconstruction strategy: A concept study on plastic models. *Comput. Biol. Med.* **111**, (2019).

48. Choplin, R. H. *et al.* Total hip arthroplasty in patients with bone defciency of the acetabulum. *Radiographics* **28**, 771–786 (2008).
49. Kawanabe, K., Akiyama, H., Goto, K., Maeno, S. & Nakamura, T. Load Dispersion Effects of Acetabular Reinforcement Devices Used in Revision Total Hip Arthroplasty. A Simulation Study Using Finite Element Analysis. *J. Arthroplasty* **26**, 1061–1066 (2011).
50. Jain, S., Grogan, R. J. & Giannoudis, P. V. Options for managing severe acetabular bone loss in revision hip arthroplasty. A systematic review. *HIP Int.* **24**, 109–122 (2014).
51. Sporer, S. M., Paprosky, W. G. & O'Rourke, M. R. Managing bone loss in acetabular revision. *Instr. Course Lect.* **55**, 287–297 (2006).
52. Chen, A. F. & Hozack, W. J. Component selection in revision total hip Arthroplasty. *Orthop. Clin. North Am.* **45**, 275–286 (2014).
53. Sporer, S. M. & Paprosky, W. G. The Use of a Trabecular Metal Acetabular Component and Trabecular Metal Augment for Severe Acetabular Defects. *J. Arthroplasty* **21**, 83–86 (2006).
54. Sheth, N. P., Nelson, C. L. & Paprosky, W. G. Femoral bone loss in revision total hip arthroplasty: Evaluation and management. *J. Am. Acad. Orthop. Surg.* **21**, 601–612 (2013).
55. Zimmer, I. Expanding options in acetabular revision surgery. *Zimmerr trabecular Met. acetabular Revis. Syst.* (2015).
56. Issack, P. S. *et al.* Acetabular component revision in total hip arthroplasty. Part II: management of major bone loss and pelvic discontinuity. *Am. J. Orthop. (Belle Mead. NJ).* **38**, 550–556 (2009).
57. Goodman, G. P. & Engh, C. A. The custom triflange cup build it and they will come. *Bone Jt. J.* **98B**, 68–72 (2016).
58. Fehring, K. A., Owen, J. R., Kurdin, A. A., Wayne, J. S. & Jiranek, W. A. Initial stability of press-fit acetabular components under rotational forces. *J. Arthroplasty* **29**, 1038–1042 (2014).
59. Adler, E., Stuchin, S. A. & Kummer, F. J. Stability of press-fit acetabular cups. *J. Arthroplasty* **7**, 295–301 (1992).
60. Weißmann, V., Boss, C., Bader, R. & Hansmann, H. A novel approach to determine primary stability of acetabular press-fit cups. *J. Mech. Behav. Biomed. Mater.* **80**, 1–10 (2018).
61. Tabata, T., Kaku, N., Hara, K. & Tsumura, H. Initial stability of cementless acetabular cups: press-fit and screw fixation interaction—an in vitro biomechanical study. *Eur. J. Orthop. Surg. Traumatol.* **25**, 497–502 (2015).
62. Goriainov, V., Jones, A., Briscoe, A., New, A. & Dunlop, D. Do the Cup Surface Properties Influence the Initial Stability? *J. Arthroplasty* **29**, 757–762 (2014).

63. Jin, Z. M. *et al.* Deformation of press-fitted metallic resurfacing cups. Part 1: Experimental simulation. *Proc. Inst. Mech. Eng. Part H J. Eng. Med.* **220**, 299–309 (2006).
64. Small, S. R. *et al.* High Initial Stability in Porous Titanium Acetabular Cups: A Biomechanical Study. *J. Arthroplasty* **28**, 510–516 (2013).
65. Shim, V., Boheme, J., Josten, C. & Anderso, I. Use of Polyurethane Foam in Orthopaedic Biomechanical Experimentation and Simulation. *Polyurethane* (2012) doi:10.5772/47953.
66. Tuwair, H., Volz, J., Elgawady, M. A., Chandrashekhara, K. & Birman, V. Modeling and Analysis of GFRP Bridge Deck Panels Filled with Polyurethane Foam. *J. Bridg. Eng.* **21**, (2016).
67. Huber, W. O. & Noble, P. C. Effect of design on the initial stability of press-fit cups in the presence of acetabular rim defects: Experimental evaluation of the effect of adding circumferential fins. *Int. Orthop.* **38**, 725–731 (2014).
68. Crosnier, E. A., Keogh, P. S. & Miles, A. W. The effect of dynamic hip motion on the micromotion of press-fit acetabular cups in six degrees of freedom. *Med. Eng. Phys.* **38**, 717–724 (2016).
69. Olory, B., Havet, E., Gabrion, A., Vernois, J. & Mertl, P. Comparative in vitro assessment of the primary stability of cementless press-fit acetabular cups. *Acta Orthop. Belg.* **70**, 31–37 (2004).
70. Naher, S., O'Callaghan, D. & Brabazon, D. A powered technique for inserting acetabular cups. *Adv. Mater. Res.* **445**, 1011–1016 (2012).
71. Milne, L. P., Kop, A. M. & Kuster, M. S. Polyaxial locking and compression screws improve construct stiffness of acetabular cup fixation: A biomechanical study. *J. Arthroplasty* **29**, 1043–1051 (2014).
72. Macdonald, W., Carlsson, L. V., Charnlcy, G. J. & Jacobsson, C. M. Press-fit acetabular cup fixation: Principles and testing. *Proc. Inst. Mech. Eng. Part H J. Eng. Med.* **213**, 33–39 (1999).
73. Weißmann, V., Ramskogler, T., Schulze, C., Bader, R. & Hansmann, H. Influence of synthetic bone substitutes on the anchorage behavior of open-porous acetabular cup. *Materials (Basel).* **12**, (2019).
74. Jin, Z. *Fundamentals of computational modelling of biomechanics in the musculoskeletal system*. *Computational Modelling of Biomechanics and Biotribology in the Musculoskeletal System: Biomaterials and Tissues* (Woodhead Publishing Limited, 2014). doi:10.1533/9780857096739.1.3.
75. Ruggiero, A., D'Amato, R. & Affatato, S. Comparison of meshing strategies in THR finite

element modelling. *Materials (Basel).* **12**, 1–11 (2019).

76. Crosnier, E. A., Keogh, P. S. & Miles, A. W. A novel method to assess primary stability of press-fit acetabular cups. *Proc. Inst. Mech. Eng. Part H J. Eng. Med.* **228**, 1126–1134 (2014).
77. Yew, A., Jin, Z. M., Donn, A., Morlock, M. M. & Isaac, G. Deformation of press-fitted metallic resurfacing cups. Part 2: Finite element simulation. *Proc. Inst. Mech. Eng. Part H J. Eng. Med.* **220**, 311–319 (2006).
78. Christian, S., Rebecca, M., Rainer, B., Daniel, K. & Holger, H. Fixation stability of uncemented acetabular cups with respect to different bone defect sizes. *J. Pre-Proof* doi:https://doi.org/10.1016/j.arth.2020.01.019.
79. Zimmer. Allofit®/Allofit®-S Alloclassic® Acetabular Cup System Surgical Technique. *Zimmer GmbH* 1–32 (2009) doi:10.1002/bjs.1800750345.
80. Zimmer, I. Trabecular Metal™ Revision Shell - Surgical Technique. *ReVision* (2008).
81. Jasty, M., Anderson, M. J. & Harris, W. H. Total hip replacement for developmental dysplasia of the hip. *Acta Orthop. Scand.* **68**, 77–84 (1995).
82. Chen, W. M., Engh, C. A., Hopper, R. H., Mcauley, J. P. & Engh, C. A. Acetabular revision with use of a bilobed component inserted without cement in patients who have acetabular bone-stock deficiency. *J. Bone Jt. Surg. - Ser. A* **82**, 197–206 (2000).
83. Li, H., Mao, Y., Oni, J. K., Dai, K. & Zhu, Z. Total hip replacement for developmental dysplasia of the hip with more than 30% lateral uncoverage of uncemented acetabular components. *Bone Jt. J.* **95 B**, 1178–1183 (2013).
84. Janssen, D., Zwartelé, R. E., Doets, H. C. & Verdonschot, N. Computational assessment of press-fit acetabular implant fixation: The effect of implant design, interference fit, bone quality, and frictional properties. *Proc. Inst. Mech. Eng. Part H J. Eng. Med.* **224**, 67–75 (2010).
85. MacKenzie, J. R., Callaghan, J. J., Pedersen, D. R. & Brown, T. D. Areas of contact and extent of gaps with implantation of oversized acetabular components in total hip arthroplasty. *Clin. Orthop. Relat. Res.* 127–136 (1994) doi:10.1097/00003086-199401000-00018.
86. Zivkovic, I., Gonzalez, M. & Amirouche, F. The effect of under-reaming on the cup/bone interface of a press fit hip replacement. *J. Biomech. Eng.* **132**, 1–8 (2010).
87. Schulze, C., Vogel, D., Sander, M. & Bader, R. Engineering Calibration of crushable foam plasticity models for synthetic bone material for use in finite element analysis of acetabular cup deformation and primary stability. *Comput. Methods Biomech. Biomed. Engin.* **0**, 1–13 (2018).
88. Souffrant, R. *et al.* Advanced material modelling in numerical simulation of primary

acetabular press-fit cup stability. *Comput. Methods Biomech. Biomed. Engin.* **15**, 787–793 (2012).

89. O'Rourke, D., Al-Dirini, R. M. A. & Taylor, M. Primary stability of a cementless acetabular cup in a cohort of patient-specific finite element models. *J. Orthop. Res.* **36**, 1012–1023 (2018).
90. Shirazi-Adl, A., Dammak, M. & Paiement, G. Experimental determination of friction characteristics at the trabecular bone/porous-coated metal interface in cementless implants. *J. Biomed. Mater. Res.* **27**, 167–175 (1993).
91. Alloclassic, A. Allofit IT Acetabular System Design Rationale. 1–16.
92. Sheth, N. P. & Della Valle, C. J. Uncemented Acetabular component. *Musculoskelet. Key* (2016).
93. Dassault Systèmes Simulia. Abaqus CAE User's Manual (6.12). *Manuals* 1174 (2012).
94. Kuhn, A., Scheller, G. & Schwarz, M. Initial stability of press-fit acetabular cups. In vitro lever-out trials. *Biomed. Tech.* **44**, 356–359 (1999).
95. Lakstein, D., Backstein, D., Safir, O., Kosashvili, Y. & Gross, A. E. Trabecular metal$^{TM}$ cups for acetabular defects with 50% or less host bone contact. *Clin. Orthop. Relat. Res.* **467**, 2318–2324 (2009).
96. Le Cann, S. *et al.* Does surface roughness influence the primary stability of acetabular cups? A numerical and experimental biomechanical evaluation. *Med. Eng. Phys.* **36**, 1185–1190 (2014).
97. O'Rourke, D. & Taylor, M. Patient and surgical variability in the primary stability of cementless acetabular cups: A finite element study. *J. Orthop. Res.* (2020) doi:10.1002/jor.24636.
98. Benzley, S. E., Perry, E., Merkley, K., Clark, B. & Sjaardema, G. A Comparison of All-Hexahedral and All-Tetrahedral Finite Element Meshes for Elastic and Elasto-Plastic Analysis. *4th Int. Meshing Roundtable, Sandia Natl. Lab.* 179–191 (1995) doi:10.1.1.70.392.
99. Tadepalli, S. C., Erdemir, A. & Cavanagh, P. R. Comparison of hexahedral and tetrahedral elements in finite element analysis of the foot and footwear. *J. Biomech.* **44**, 2337–2343 (2011).
100. Kheir, M. M. *et al.* Complications of total hip arthroplasty. *Orthop. Knowl. Updat. Hip Knee Reconstr. 5* **27**, 472–505 (2018).
101. Raffa, M. L. *et al.* Dependence of the primary stability of cementless acetabular cup implants on the biomechanical environment. *Proc. Inst. Mech. Eng. Part H J. Eng. Med.* **233**, 1237–1249 (2019).

# Appendix A

*Figure A.1 - Allofit® and TM™ cups after the insertion in the PU-foam block. Allofit® shell in the 90/45 defect block on the left and TM™ shell in the120/45 defect on the right.*

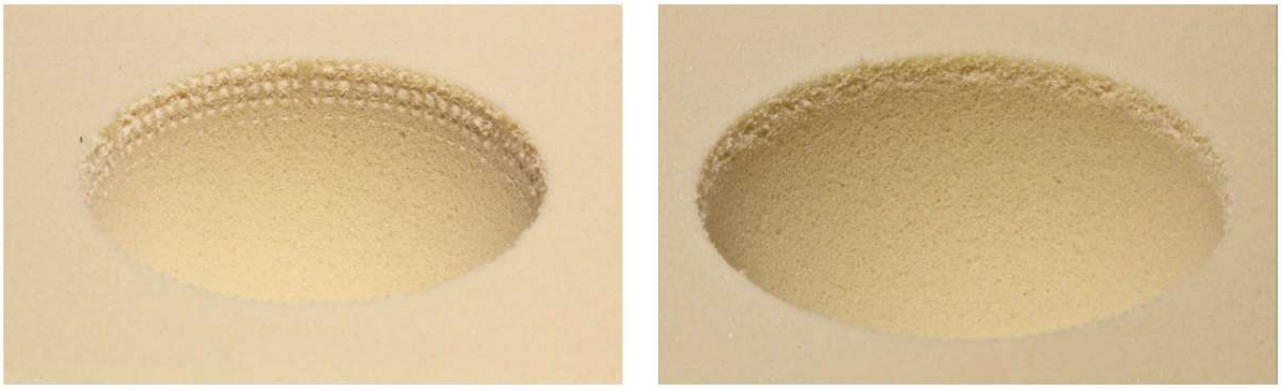

*Figure A.2 - Intact cavity block after the cups extraction: Allofit® (left), TM™ (right).*

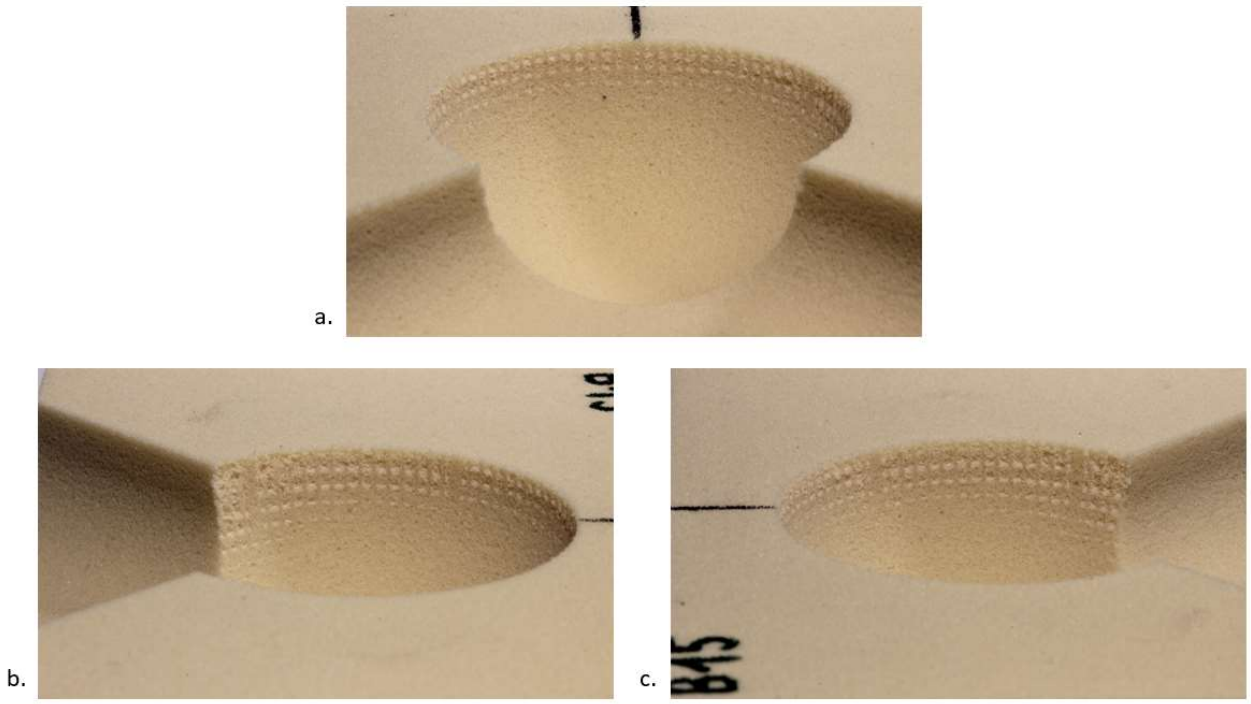


*Figure A.3 - Defect 90/45 block after Allofit® extraction: a. front view, b. left view, c. right view.*

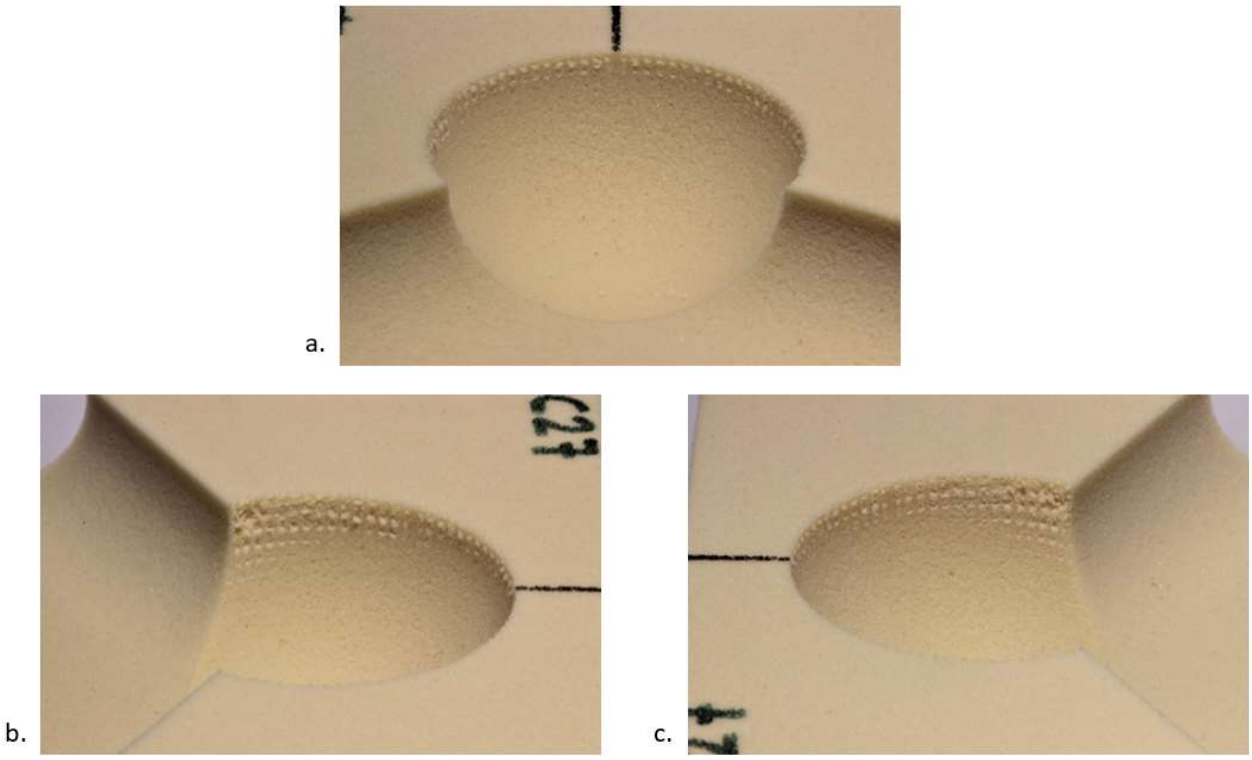


*Figure A.4 - Defect 120/45 block after Allofit® extraction: a. front view, b. left view, c. right view.*

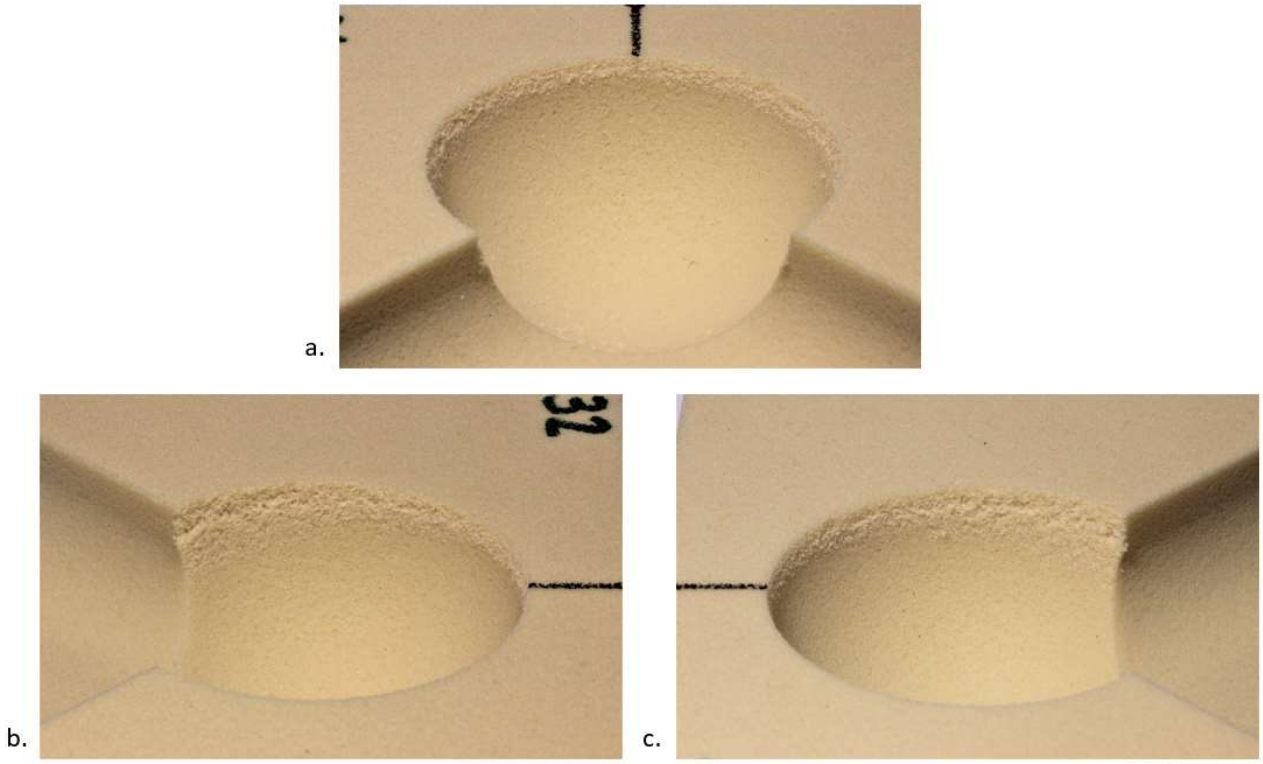


*Figure A.5 - Defect 90/45 block after TM™ extraction: a. front view, b. left view, c. right view.*

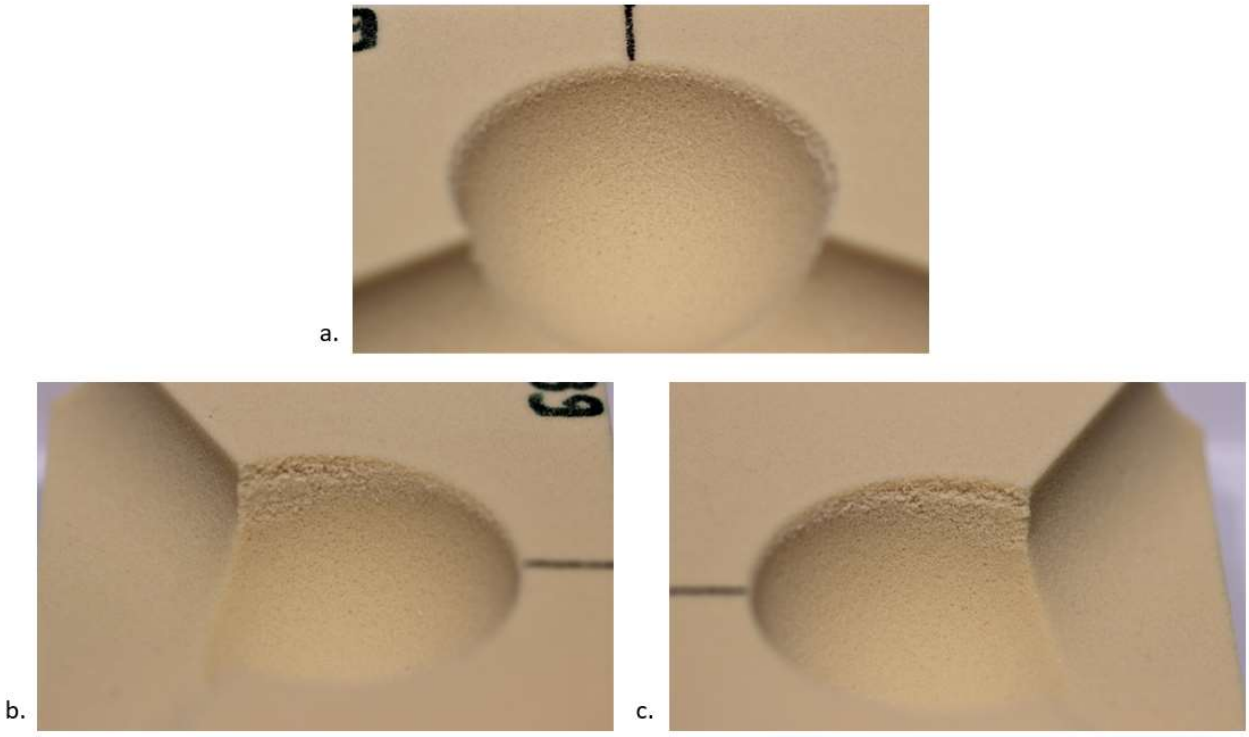


*Figure A.6 - Defect 120/45 block after TM™ extraction: a. front view, b. left view, c. right view.*

# Figure index